BULLETIN OF BIOTECHNOLOGY

e-ISSN: 2717-8323

Cilt: 5 Volume: 1 Year: 2024

BULLETIN OF BIOTECHNOLOGY

Cilt: 5 Volume: 1 Year: 2024

Published Biannually

Corresponding Address
Karamanoğlu Mehmetbey University, Faculty of Health, Sciences, Department of Nutrition and Dietetics, Karaman, Türkiye
E-mail: mtdogan1@gmail.com
Web: https://www.dergipark.org.tr/biotech

Owner / Publisher
Assoc. Prof. Dr. Muhammet DOĞAN
This journal is peer-reviewed and published twice (June, December) a year.

e-ISSN 2717-8323

BULLETIN OF BIOTECHNOLOGY

e-ISSN 2717-8323

Cilt: 5 Volume: 1 Year: 2024

Contents

Research Articles

RESEARCH ARTICLE
Bull Biotechnol (2024) 5(1):1-6
https://doi.org/10.51539/biotech.1393136 Journal homepage: www.dergipark.org.tr/biotech

Bulletin of Biotechnology

Starches as solidifiers for medicinal plant micropropagations and biomass accumulations

Pınar Nartop[1*], Melis Aylin Fındıkoğlu[1], Meltem Taştekin[1]

[1]*Department of Biomedical Engineering, Faculty of Engineering, Tekirdağ Namık Kemal University, 59860, Çorlu, Tekirdağ, Turkey*

*Corresponding author : pnartop@nku.edu.tr
Orcid No: https://orcid.org/0000-0003-2765-6133

Received : 19/11/2023
Accepted : 12/01/2024

To Cite: Nartop P, Fındıkoğlu MA, Taştekin M (2024) Starches as solidifiers for medicinal plant micropropagations and biomass accumulations. Bull Biotechnol 5(1):1-6 https://doi.org/10.51539/biotech.1393136

Abstract: In plant tissue and cell culture studies, media compositions are one of the most important factors affecting the micropropagation procedure's efficiency. Micropropagation studies can be conducted for commercial productions of medicinal plants, and low-cost options always have significance in large-scale productions. Some media component substitutes have been studied to reduce production costs. Agar, the media solidifier, is one of the most expensive components of media compositions. In this study, corn and wheat starches were used as media solidifiers at 80 and 100 g/L concentrations, and their effects on plant growth (shoot elongations, shoot, node, and root numbers) and biomass accumulations (shoot and root fresh and dry weights) in *Lavandula officinalis* and *Digitalis purpurea* node cultures were reported. The results showed that starch type and their concentrations significantly affected plant growth. Maximum multiple shoot number was recorded in medium supplemented with 80 g/L starch and was 61.3% higher than the control. Biomass accumulations were not statistically significant; however, higher biomass accumulations were detected in starch-added media than in control. Consequently, corn and wheat starches can be used at these concentrations as a substitute for agar to induce multiple shoot formations in *L. officinalis* and *D. purpurea* node cultures.

Keywords: *Lavandula officinalis*; *Digitalis purpurea*; Starch; Micropropagation; Biomass accumulation

1 Introduction

Plant tissue culture techniques are one of the most popular and efficient ways of producing a high-yield biomass production of high-quality medicinal plants (Moraes et al. 2021). Plant tissues and plantlets can be grown homogenously under controlled conditions in laboratories without the effects of external conditions. High biomass accumulation is needed, as plant cells are biofactories that produce plant secondary metabolites, which are frequently utilized in the pharmaceutical, food, and textile industries. In order to increase biomass accumulation in plant tissue cultures, media compositions such as concentrations of macro- and microelements, growth regulators, and vitamins should be optimized first (Nartop 2018). The concentration of agar, which is essential for the solidification of culture media, is also essential. 6-7 g/L agar is generally added to the culture medium to prepare semi-solid media. However, the price of agar is the primary parameter that determines the cost of production, as it is the most expensive component of culture medium (Tyagi et al. 2007). In order to substitute agar, researchers use different and low-cost solidifiers such as herbal flours, starches, guar gum, isabgol-husk, and sago powder at different concentrations (Daut et al. 2011; Gour and Kant 2011; Özkaynak et al. 2016).

Digitalis purpurea L. (*Scrophulariaceae*) is a medicinal plant, and treatment with drugs based on *Digitalis* extracts is frequently used to strengthen cardiac diffusion and regulate heart rhythm. Digitoxin, digoxin, and lanatoside C are the cardiac glycosides extracted from the leaves of *D. purpurea* plants. The contents of these glycosides are affected when traditional agricultural methods obtain biomass production. Therefore, *in vitro* biomass production can be a better and more beneficial method to avoid the effects of climatic and soil conditions (Bourgaud et al. 2001; Roca-Perez et al. 2004).

Lavandula officinalis L. (*Lamiaceae*) (lavender) is an aromatic and medicinal plant used for its therapeutic properties since ancient times. The main components of the aerial parts and flowers are linalool, linalyl acetate,

monoterpenes, sesquiterpenes, flavonoids, and terpenoids. The extracts obtained from the plant have a sedative effect on the central nervous system and trigger memory and learning. Essential oil of lavender is also used for its antimicrobial, antibacterial, antitumor, anti-inflammatory, antihistaminic, and antidiabetic effects (Alnamer et al. 2012; Rabiei et al. 2014; Raisi et al. 2020).

Because of their valuable pharmacological activities, these two plants are always of interest to medicinal plant producers. Therefore, micropropagation of these valuable medicinal plants offers a standard production method, independent of climatic and soil conditions, which are important for commercial production, especially for the pharmaceutical industry. In our study, a low-cost micropropagation method, depending on starches as medium solidifiers, was investigated; nodes obtained from *in vitro*-grown *D. purpurea* and *L. officinalis* plantlets were cultivated in WPM media containing agar (control – 6 g/L), wheat and corn starches (80 and 100 g/L) to determine their physiologic effects on growth parameters and biomass production rates.

2 Materials and Method

2.1 Plant Material and Culture Conditions

Sterile *L. officinalis* and *D. purpurea* shoots, micropropagated from nodal explants and grown in WPM medium, were transferred to media given in Table 1. Node cultures of each species were cultivated for four weeks at 16 h photoperiod (4000 lux) and 24±1°C temperature to investigate the effects of wheat and corn starches on growth parameters and biomass production of *L. officinalis* and *D. purpurea*.

Table 1. Media composition used for *L. officinalis* and *D. purpurea* micropropagation.

Media	Basal Medium	Agar	Wheat Starch	Corn Starch	Sucrose	pH
Control	WPM	6 g/L	-	-	30 g/L	5.8
B80	WPM	-	80 g/L	-	30 g/L	5.8
B100	WPM	-	100 g/L	-	30 g/L	5.8
M80	WPM	-	-	80 g/L	30 g/L	5.8
M100	WPM	-	-	100 g/L	30 g/L	5.8

Woody plant medium (Lloyd and McCown 1980) (WPM) supplemented with 6 g/L agar and 30 g/L sucrose was used as basal medium. Other media were derived from WPM medium and contained different concentrations of wheat (80 and 100 g/L) and corn (80 and 100 g/L) starches. The pH of the media was adjusted to 5.8. The media were autoclaved at 121°C and a pressure of 1.2 kg/cm^2 for 15 mins before use.

In the fourth week of cultivation, all cultures were terminated. After plantlets were removed from culture vessels, their bottom parts and roots were cleared from agar with the help of a napkin. *In vitro*-grown shoots and roots were distinguished from each other, and their fresh weights were recorded. These shoots and roots were dried for seven days at room temperature (24±1°C), and their dry weights were recorded.

2.2 Growth Parameters

Growth parameters were determined as shoot elongations (SE), node numbers (NN), root numbers (RN), shoot numbers (SN), multiple shoot numbers (MSN), and biomass accumulations were specified as shoot fresh weights (SFW), shoot dry weights (SDW), root fresh weights (RFW) and root dry weights (RDW).

2.3 Statistical Analysis

The study was implemented in a factorial randomized plot design, and each experiment was repeated thrice. Fifteen explants were used for each replicate. Data were analyzed with ANOVA, and the post hoc tests were performed using the Tukey test at $p < 0.05$.

3 Results

All the node explants used in this study turned into plantlets, and their roots started to grow in the second week of the culture period. In Table 2, the results were given by means of the growth parameters and biomass accumulation.

SE was detected higher on *L. officinalis* (1.90 cm) than *D. purpurea* (1.17 cm). The highest SE was observed on *L. officinalis at* 3.21 cm in B100. The highest SE of *D. purpurea* was 1.87 in M100, which was 49.6% higher than the control. The interaction between plant and starch types was statistically significant (p=0.024), and the highest value was detected in *L. officinalis**wheat starch interaction (2.26 cm). Even though there was no statistical significance, the mean results of SE showed that wheat starch was found more beneficial than corn starch (Table 2c), and the use of 100 g/L starch had the highest SE (Table 2d), which was 50.4% higher than the control.

The highest NN was detected (9.62) on *L. officinalis* in the B100 medium, whereas the highest NN on *D. purpurea* was observed in the M80 medium (3.53) (Table 2a). The interaction between plant type and media was statistically significant (p=0.049), and the highest value was detected on *L. officinalis**100g (8.76). The effect of starches on mean NN was nearly the same: 4.43 in wheat starch and 4.44 in corn starch (Table 2c). Similar to SE, 100 g/L starch had the highest value in NN (5.16), which was 52.7% higher than the control (3.38) (Table 2d).

Table 2. (a) Shoot elongation (SE), node (NN), root (RN), shoot (SN) and multiple shoot numbers (MSN) of *L. officinalis* and *D. purpurea* in media supplemented with wheat and corn starch at 80 g/L and 100 g/L concentrations **(b)** Mean values of plant type **(c)** Mean values of starch type **(d)** Mean values of media.

Table 2a

Plant	Media	SE (cm)	NN	RN	SN	MSN
Lavandula officinalis	Control	1.23±0.22	5.64±1.54	1.05±0.41	1.73±0.22	16.30±3.92
	B80	2.36±0.34	6.71±0.94	1.16±0.10	2.07±0.33	48.89±14.59
	B100	3.21±0.43	9.62±0.43	1.67±0.17	2.82±0.21	26.67±1.29
	M80	1.99±0.55	6.93±1.36	2.24±0.33	2.38±0.55	21.48±7.53
	M100	1.38±0.73	7.89±0.79	3.13±0.44	1.87±0.61	17.04±4.13
Digitalis purpurea	Control	1.25±0.49	1.11±0.34	2.38±0.97	0.56±0.14	6.67±2.23
	B80	0.64±0.16	1.93±0.34	2.42±0.81	0.51±0.12	0.74±0.74
	B100	0.97±0.11	1.55±0.40	3.00±0.20	0.78±0.22	5.18±1.96
	M80	1.06±0.12	3.53±0.93	3.71±0.61	0.80±0.19	2.96±1.96
	M100	1.87±0.61	1.56±0.50	3.73±0.62	1.06±0.24	7.41±1.96

Table 2b

Plant Type	SE (cm)	NN	RN	SN	MSN
Lavandula officinalis	1.90 A	7.07 A	1.71 B	2.10 A	24.44
Digitalis purpurea	1.17 B	1.80 B	2.94 B	0.71 B	4.94
p	0.006	0.001	0.001	0.001	0.001

Table 2c

Starch Type	SE (cm)	NN	RN	SN	MSN
Wheat	1.60	4.43	1.94 B	1.41	17.41
Corn	1.46	4.44	2.71 A	1.40	11.98
p	0.553	0.976	0.031	0.950	0.090

Table 2d

Media	SE (cm)	NN	RN	SN	MSN
Control	1.23	3.38 B	1.71 B	1.15	11.48
80g	1.51	4.77 AB	2.38 AB	1.44	18.52
100g	1.85	5.16 A	2.88 A	1.63	14.07
p	0.139	0.026	0.028	0.098	0.189

Each value is the mean of 3 replications, each with 15 explant. Values within column followed by different letters are significantly different at the 0.05 level by the Tukey test.

RN was affected significantly by plant type (p=0.001), starch type (p=0.031), and media (p=0.028). The highest RN was observed in M100 (3.73) on *D. purpurea*, whereas the highest RN on *L. officinalis* (3.13) was detected in the same medium as well (Table 2a). The mean RN (Table 2c) was higher for corn starch (2.71) than wheat starch (1.94). The results showed that corn starch had better effects on root growth than wheat starch. Once again, similar to SE and NN, 100 g/L starch concentration had the highest RN value (2.22), which was 30% higher than the control (1.71) (Table 2d).

In SN, only plant type was statistically significant. The highest SN (2.82) was obtained in B100 on *L. officinalis*. The maximum SN on *D. purpurea*was 1.06 in M100 (Table 2a). As such, in NN, the effects of starches on mean SN were nearly the same: 1.41 in wheat starch and 1.40 in corn starch (Table 2c). 100 mg/L starch concentration was the highest (1.63) and 42% higher than the control (1.15) (Table 2d).

The interactions between plant type*media and plant type*starch type were found statistically significant for MSN (p=0.012 and p=0.034, respectively). The maximum values for MSNs were detected in *L. officinalis**80g interaction (35.19) and *L. officinalis**wheat starch interaction (30.62). However, in *D. purpurea*, corn starch was more beneficial than wheat starch (5.67 and 4.20, respectively). The mean values were higher in wheat than in corn starch (Table 2c). 80 g/L starch concentration (Table 2d) had the highest MSN and was 61.3% higher than the control.

Table 3: (a) Shoot fresh (SFW) and dry (SDW) weights, root fresh (RFW) and dry (RDW) weights of *L. officinalis* and *D. purpurea* in media supplemented with wheat and corn starch at 80 g/L and 100 g/L concentrations **(b)** Mean values of plant type **(c)** Mean values of starch type **(d)** Mean values of media.

Table 3a

Plant	Media	SFW (g)	SDW (g)	RFW (g)	RDW (g)
Lavandula officinalis	Control	1.14±0.30	0.18±0.04	0.52±0.21	0.03±0.01
	B80	0.76±0.04	0.16±0.02	0.17±0.06	0.03±0.01
	B100	0.71±0.02	0.13±0.01	0.31±0.15	0.04±0.01
	M80	0.83±0.19	0.16±0.04	0.58±0.09	0.09±0.01
	M100	0.80±0.08	0.14±0.01	0.61±0.05	0.11±0.01
Digitalis purpurea	Control	1.33±0.25	0.13±0.04	0.71±0.49	0.04±0.02
	B80	0.92±0.23	0.15±0.05	0.80±0.23	0.11±0.04
	B100	0.62±0.09	0.09±0.01	1.18±0.69	0.20±0.10
	M80	1.53±0.21	0.16±0.03	2.29±0.19	0.26±0.03
	M100	1.56±0.54	0.15±0.05	1.08±0.46	0.14±0.06

Table 3b

Plant Type	SFW (g)	SDW (g)	RFW (g)	RDW (g)
Lavandula officinalis	0.90 B	0.16	0.44 B	0.05 B
Digitalis purpurea	1.21 A	0.13	1.14 A	0.18 A
p	0.037	0.237	0.001	0.005

Table 3c

Starch Type	SFW (g)	SDW (g)	RFW (g)	RDW (g)
Wheat	0.91	0.14	0.61	0.08
Corn	1.20	0.15	0.97	0.15
p	0.059	0.473	0.078	0.075

Table 3d

Media	SFW (g)	SDW (g)	RFW (g)	RDW (g)
Control	1.23	0.15	0.63	0.05 B
80g	1.01	0.15	0.95	0.12 AB
100g	0.92	0.13	0.79	0.18 A
p	0.211	0.460	0.405	0.038

Each value is the mean of 3 replications, each with 15 explant. Values within the column followed by different letters are significantly different at the 0.05 level by the Tukey test.

In SFW, plant type was detected as statistically significant (p=0.037). The maximum SFW of *L. officinalis* was obtained in control (1.14 g), whereas 1.56 g of SFW was the maximum value for *D. purpurea* in M100 (Table 3a). In SDW, no statistical significance was detected amongst the parameters tested. The maximum SDWs for *L. officinalis* and *D. purpurea* were 0.18 g in control and 0.16 g in M80, respectively. Starch-type values were detected nearly the same (Table 3c).

RFW values were only statistically significant for plant type (p=0.001) (Table 3b). The maximum RFWs for *L. officinalis* and *D. purpurea* were were 0.61 g in M100 and 2.29 g in M80, respectively (Table 3a). The mean RFW values were higher in corn starch (0.97 g) than in wheat starch (0.61 g) (Table 3c). The highest mean RFW (0.95 g) was detected in 80g (Table 3d). RDW values were affected significantly by plant type (Table 3b) and media (p=0.005 and p=0.038, respectively). The maximum RDWs for *L. officinalis* and *D. purpurea* were 0.11 g in M100 and 0.26 g in M80, respectively. Corn starch had a higher biomass accumulation effect on mean RDW than wheat starch (0.15 g and 0.08 g, respectively) (Table 3b). The highest mean RDW was detected at 100g (0.18 g), which was 3.6 times higher than the control (0.05 g) (Table 3d).

4 Discussion

The first examinations of the starches' effects were done visually. Both corn and wheat starches at 80 and 100 g/L concentrations gave enough strength to the culture medium to place the node explants easily and support growth. Similarly, Ebile et al. (2022) reported no morphological or vitrification problems when banana shoots were cultivated in a medium supplemented with tapioca starch instead of agar.

SE values of *L. officinalis* were found to be higher in media supplemented with starches than in the control. In *D. purpurea*, only M100 values were higher than in the control. Wheat starch showed higher SEs on plantlets (Table 2c). The use of 100 g/L starch concentration had the highest SE. Corn and wheat starches have promoted elongations of shoots in both plant types in our study (Table 2d). Similarly, Özkaynak et al. (2016) reported the use of guar gum, a plant-based natural product, as a medium solidifier, and the results showed that plant height in *in vitro* cultures of *Solanum tuberosum* was enhanced from 5.9 cm to 7.76 cm when guar gum was added to MS medium at 12 g/L.

NN values showed an accordance with SE values as expected. The type of starch did not affect the NN. However, 100 g/L concentration had the highest NN and was 52.6% higher than the control. The number of nodes per explant was also enhanced in *S. tuberosum in vitro* cultures when 15 g/L guar gum was added to the MS medium (Özkaynak et al. 2016).

The number of roots in both plant types was higher than the control in starch-applied media. RNs of both plant types gradually increased as the starch concentration enhanced. RNs of corn starch-added media were higher than those of wheat starch-added media. This result showed that corn starch can be preferred in root culture studies, and 100 g/L concentration will benefit better root growth.

In micropropagation studies, one of the most critical parameters is the multiple shoot formation rate. High numbers of multiple shoot formations facilitate micropropagation and accelerate biomass accumulations. Therefore, the component that triggers the multiple-shoot formation should be specified. In our study, MSN values were affected by plant type*media and plant type*starch interactions. Interestingly, *L. officinalis* was mainly affected by wheat starch, whereas corn starch was more effective on *D. purpurea*. Daud et al. (2011) reported that potato starch was used effectively at 40-100 g/L concentrations in *Celosia* sp. stem cultures as the jelling agent, and the number of shoot regenerations was detected between 18.90 and 26.50. In some micropropagation studies, starches and agar were used together in culture media. The results showed that using lower amounts of agar (1-2 g/L) when combined with starches, enhanced the number of shoot regenerations (Karim et al. 2003; Mohamed et al. 2009; Daud et al. 2011). This result may be the consequence of the structure of the starches; they are carbohydrates and may act as carbon sources in culture conditions for plant explants for their better growth. Hence, different starches can be used alone or with agar in culture media to promote the rate of micropropagation via enhanced multiple-shoot formations.

Biomass accumulation is important for micropropagation studies, especially in producing valuable medicinal plants. Our study evaluated fresh and dry weights of shoots and roots. Although no statistical significance was detected in starch type and media experiments, corn starch had higher mean results among these four parameters. Hence, corn and wheat starches can be used instead of agar because of the lack of statistical significance between the parameters. However, different starches can be used to promote biomass accumulation. Özkaynak et al. (2016) reported that using 18 and 20 g/L guar gum in MS medium enhanced fresh weights in *S. tuberosum* from 0.71 g to 1.68 g and 1.12 g, respectively.

Different materials were used instead of agar for different plant and culture types. Jain and Babbar (2006) successfully used xanthan gum as a media solidifier in *Calliandra tweedii in vitro* cultures to obtain seed germination, caulogenesis and somatic embryogenesis. Interestingly, Deb and Pongener (2010) used polyurethane foam discs, chopped coconut and betel nut coirs and leaf litters instead of agar in order to obtain *in vitro* seed germination and plant regeneration of *Cymbidium aloi* and the best results were obtained from polyurethane foam. Moraes-Cerdeira et al (1995) reported that cotton fibers utilized for callus maintenance and shoot organogenesis of *Agrostis* and *Taxus* were found better than agar.

5 Conclusion

Using starches as media solidifiers is an essential low-cost option for micropropagation studies. The prizes of the starches are much lower than the agar prizes. Starches have been mainly used in nourishment. Therefore, they are easy to access. Moreover, their plant-based and non-toxic (edible) nature positively affects plant growth in *in vitro* conditions. They support plant explants in media as both media solidifiers and carbon sources. This study proved that corn and wheat starches did not show toxic or growth-inhibiting effects on *L. officinalis* and *D. purpurea* node cultures. Multiple shoot formations, which strongly affect the micropropagation rate, were promoted by 80 and 100 g starch additions. These results showed that more studies should be established about media solidifiers, which may be substituted for agar.

Acknowledgements

This study was not supported by a project or company.

Authors' contributions:

PN: Study conception, design, supervision, data analysis, tatistical analysis, literature review, manuscript writing, editing and laboratory experiments
MAF: Laboratory experiments
MT: Laboratory experiments

Conflict of interest disclosure:

The authors declare no conflict of interest.

References

Alnamer R, Alaoui K, Bouidida EH, Benjouad A, Cherrah Y (2012) Sedative and hypnotic activities of the methanolic and aqueous extracts of *Lavandula officinalis* from Morocco. *Adv Pharmacol Sci 5*. http://doi.org/10.1155/2012/270824.

Bourgaud F, Gravot A, Milesi S, Gontier E (2001) Production of Plant Secondary Metabolites: A Historical Perspective. *Plant Sci 161*:839-851. https://doi.org/10.1016/S0168-9452(01)00490-3

Daud N, Taha RM, Mohd NN, Alimon H (2011) Potential of alternative gelling agents in media for the *in vitro* micro-propagation of *Celosia* sp. *Int J Bot 7(2):*183-188. https://doi.org/10.3923/ijb.2011.183.188

Deb CR, Pongener A (2010) Search of alternative substratum for agar in plant tissue culture, Curr Sci 98(1):99-102.

Ebile PA, Opata J, Hegele S (2022) Evaluating suitable low-cost agar substitutes, clarity, stability, and toxicity for resource-poor countries' tissue culture media. In Vitro Cell Dev Biol – Plant 58:989-1001. https://doi.org/10.1007/s11627-022-10285-6.

Gour VS, Kant T (2011) Efficacy of low cost gelling agents and carbon source alternatives during *in vitro* rooting of *Balanites aegyptiaca* and *Phyllanthus emblica* microshoots. Tree Forest Sci Biotechnol *5(1):*58-60.

Jain R, Babbar SB (2006) Xanthan gum: an economical substitute for agar in plant tissue culture media. Plant Cell Rep 25:81–84. https://doi.org/10.1007/s00299-005-0039-8

Karim MZ, Amin MN, Azad MAK, Begum F, Rahman MM, Ahmad S, Alam R (2003) *In vitro* shoot multiplication of *Chrysanthemum morifolium* as affected by sucrose, agar and pH. Biotechnol 2, 115-120. https://doi.org/10.3923/biotech.2003.115.120

Lloyd GB, McCown BH (1980) Commercial-feasible micropropagation of mountain laurel- *Kalmia latifolia* by use of shoot- tip culture. Proc Int Plant Prop Soc 30:421–427.

Mohamed MAH, Alsadon AA, Al-Mohaidib MS (2009) Corn and potato starch as an alternative for *Solanum tuberosum* micropropagation. Afr J Biotechnol *8*:9199-9203. https://doi.org/10.5897/AJB09.638

Moraes RM, Cerdeira AL, Lourenco MV (2021) Using micropropagation to develop medicinal plants into crops. Molecules 26(6):1752.

Moraes-Cerdeira RM, Krans JV, McChesney JD, Pereira AMS, Franca SC (1995) Cotton fiber as a substitute for agar support in tissue culture. HortScience 30(5):1082-1083. https://doi.org/10.21273/HORTSCI.30.5.1082

Nartop P (2018) Engineering of Biomass Accumulation and Secondary Metabolite Production in Plant Cell and Tissue Cultures, Plant Metabolites and Regulation Under Environmental Stress, (eds.) Parvaiz Ahmad, Mohammad Abass Ahanger, Vijay Pratap Singh, Chapter 9, Elsevier, pp. 169-194, ISBN: 978-0-12-812689-9. https://doi.org/10.1016/B978-0-12-812689-9.00009-1

Özkaynak E, Yüksel F, Erüst N, Şimşek T (2016) Effect of using gelling agent guar gum and different sugar sources on potato micropropagation. Turk J Agr Nat Sci 3(4):249-254.

Rabiei Z, Rafieian-Kopaei M, Makhtari S, Alibabaei Z, Shahrani M (2014) The effect of pretreatment with different doses of *Lavandula officinalis* ethanolic extract on memory, learning and nociception. Biomed Aging Pathol 4(1):71-76. https://doi.org/10.1016/j.biomag.2013.10.006

Raisi A, Davoodi F, Afshar-Ghahremani S, Taheri S, Sharifi S, Adel M (2020) Evaluation of the anesthetic and tranquilizing effects of clove powder (*Syzygium aromaticum*) and lavender oil (*Lavandula officinalis*) in convict cichlid fish (*Cichlasoma nigrofasciata*). Iran J Vet Surg 15(1):1-7. https://doi.org/10.30500/IVSA.2019.193913.1191

Roca-Perez L, Boluda R, Gavidia I, Perez-Bermudez P (2004) Seasonal cardenolide production and Dop5βr gene expression in natural populations of *Digitalis obscura*. Phytochem 65:1869-1878. https://doi.org/10.1016/j.phytochem.2004.05.004

Tyagi RK, Agrawal A, Mahalakshmi C, Hussain Z, Tyagi H (2007) Low-cost media for *in vitro* conservation of turmeric (*Curcuma longa* L.) and genetic stability assessment using RAPD markers. In Vitro Cell Dev Biol– Plant 43:51-58.

RESEARCH ARTICLE
Bull Biotechnol (2024) 5(1):7-10
https://doi.org/10.51539/biotech.1408472 Journal homepage: www.dergipark.org.tr/biotech

Bulletin of Biotechnology

Investigation of the genetic defects of Cholesterol deficiency and Brachyspina syndrome in Holstein breed cattle reared in Eskişehir

Beste Goneci[1], Muhammet Kaya[1*]

[*1]*Department of Agicultural Biotechnology, Faculty of Agriculture, Eskisehir Osmangazi University, Eskisehir, Turkey*

*Corresponding author : muhammetkaya@ogu.edu.tr
Orcid No: https://orcid.org/0000-0001-6474-121X

Received : 22/12/2023
Accepted : 04/03/2024

To Cite: Goneci B, Kaya M (2024) Investigation of the genetic defects of Cholesterol deficiency and Brachyspina syndrome in Holstein breed cattle reared in Eskişehir. Bull Biotechnol 5(1):7-10 https://doi.org/10.51539/biotech.1408472

Abstract: As a result of the intensive use of biotechnology in cattle breeding, the incidence of rare genetic defects in the population has started to increase. Studies have focused on identifying cattle with genetic defects using molecular methods. Identifying carrier cattle is crucial to reducing genetic defects in future generations. In a previous study conducted in Turkiye, Brachyspina Syndrome (BS) and Cholesterol Deficiency (CD) were detected in Holstein cattle. With regard to these two genetic defects, in the study conducted to investigate samples were taken from the Holstein cattle reared in Eskişehir by using PCR technique. 2 and 11 cattle were found to be carriers of the BS and CD, respectively, among 112 Holstein cattle. The possibility of the spread of genetic defects and economic damage can be prevented using molecular techniques. Some molecular methods can be used to detect genetic diseases. In this way, herds free of genetic defects can be produced.

Keywords: *ABOP*, Cholesterol Deficiency, *FANCI*, Brachyspina Syndrome, Holstein

1 Introduction

Genetic diseases in cattle can result in substantial economic losses. Early detection of genetic defects is crucial for eliminating carriers from the breeding program. Recent technological advancements have led to the discovery of new genetic diseases and their detection. The recessive and genetic diseases Brachyspina Syndrome (BS) and Cholesterol Deficiency (CD) were identified in 2006 (Agerholm vd. 2006) and 2015 (Kipp vd. 2015) respectively.

Autosomal recessive diseases occur when functional changes happen in both pairs of genes at the same location. This type of inherited disease does not occur in every generation. Many genetic diseases in cattle are the result of autosomal recessively inherited genes. Autosomal recessive alleles spread unnoticed as they cannot be identified by external appearance in heterozygous inheritance (Agerholm 2007). OMIA reports that there are 630 diseases in cattle, of which 73 affect the Holstein breed (OMIA 2023).

BS was documented for the first time in 2006 (Agerholm et al. 2006). To date, it has been found in the Netherlands (Agerholm and Peperkamp 2007), Italy (Testoni et al. 2008), Germany (Buck et al. 2010), and Canada (Agerholm et al. 2010). BS is a rare inherited disease in Holstein cattle. The mutation that causes BS is located in the Fanconi anemia complementation group 1 (*FANCI*) gene (OMIA 2023). A deletion of 3329 bp in the *FANCI* on the 21st chromosome is the cause of the genetic disorder in cattle (Charlier et al. 2012). Due to mutation, the *FANCI* gene contains a prematüre stop codon in exon 28, resulting from a frameshift deletion from exon 25 to 27 of the original 37 exons (Li et al. 2016). As in the first case, these two stillborn calves had long legs and short bodies. Various abnormalities were also observed in the autopsy findings examined radiographically (Testoni et al. 2008). Apart from these cases, dead Holstein calves with identical phenotype and morphological signs have been reported in the Netherlands (Agerholm and Peperkamp 2007), Germany (Buck et al. 2010), and Canada (Agerholm et al. 2010). In Poland, in a study of 78 Holstein cattle by Ruść and Kamiński (2015), 8 out of 78 animals were carriers. In China, when 342 cattle born between 1996 and 2012 were screened by Li et al. (2016), 13 were found to be carriers. In 2021, a study was conducted on 250 Holstein cattle in Turkiye to test

for BS. One of the cattle was identified as a carrier (Bedir Dibıc, 2021).

The genetic CD defect was first detected in a bull named Mauglin Storm, born in 1991 (Menzi et al. 2016). As bulls descended from Mauglin Storm are used in artificial insemination, the frequency of the mutant allele causing the hereditary defect of CD has increased in many countries. Calves with homozygous inheritance of the defect showed signs of hypolipidemia and hypocholesterolemia. The CD leads to early death due to a 1.3 kb insertion in the 5th exon of the apolipoprotein B (*APOB*) gene on the 11th chromosome of BTA (*Bos taurus autosomal*), which affects lipid metabolism (Schutz et al. 2016). *APOB* is the structural chylomicron protein of low (LDL) and very low (VLDL) density lipoproteins (Kane et al. 1980). The resulting 1.3 kb insertion creates a stop codon in the open reading frame (ORF) of *APOB*. As a result, the protein is much shorter than its 140 amino acid length. In heterozygous animals may not show any symptoms, but the genetic defect may become apparent as they age. It has been observed that animals with a homozygous genotype for CD cannot excrete chylomicrons in the intestine at an early age. This indicates a problem in the cholesterol absorption stream, as shown in the study by Schütz et al. in 2016. After checking the Mauglin Storm pedigree, 27 Holstein cattle were selected in Poland, of which 9 were found to be carriers of the genetic disease CD. These results suggest that the mutation causing the genetic disease CD is also transmitted to Holstein cattle in Poland (Kamiński and Ruść 2016). A study was conducted in Switzerland with 254 Holstein cattle to investigate the effect of the *ABOP* genotype on cholesterol metabolism. The study revealed that none of the 254 Holstein cattle had a homozygous affected genotype. Out of the total, 36 were found to be carriers, while 218 had normal alleles. Of the 1,817 Russian cattle born in Russia between 2010 and 2017, a sample of 147 was randomly selected and found to carry the defect. A study was conducted in Turkiye in 2021 to test 250 Holstein cattle for carriers. Out of the 250 cattle tested, four were found to be carriers. The study found a low frequency of the genetic disease in Holstein cattle bred in Turkiye (Bedir Dibıc 2021).

The genetic defects of BS and CD, identified in cattle populations in different countries, were investigated in the Holstein cattle population reared in Eskişehir. PCR was employed to investigate two genetic defects in the Holstein breed to ensure healthier herds in Eskişehir.

2. Materials and Method

The study was conducted at the Molecular Genetics Laboratory, which is part of the Department of Agricultural Biotechnology, Faculty of Agriculture, Eskişehir Osmangazi University. The research involved the isolation of genomic DNA molecules from blood samples, PCR amplification of regions related to inherited defects, and interpretation of electrophoresis band patterns generated by PCR products in terms of genetic defects.

2.1 Material

Blood samples were collected from 112 cows from 4 different Holstein farms in Eskişehir. The study material consisted of 25 animals from each of the three farms, and 37 animals from the fourth farm. The age of the cows in the study was changing from 3 to 5 years old.

Genomic DNA was isolated from the blood samples using the commercial kit and stored at 4°C.

2.2 Methods

In the study, 112 blood samples were collected from animals and stored in 5 mL EDTA tubes at -20°C until DNA isolation. DNA was isolated from the blood using commercial kits (PureLink DNA Isolation Kit for Genomic DNA). After isolating the DNA, we checked the samples using agarose gel electrophoresis. The genotypes for BS and CD were determined using PCR.

The PCR reaction mixture (20 µl) contained 50–100 ng DNA template, 10X Taq polymerase buffer, 1.5 mM MgCl2, 2.5 mM dNTPs, 0.5 U Taq DNA polymerase and 5 pmoles of each primer (Table) per reaction. The PCR cycle profile was 94°C for 3 min; then 35 cycles of 94°C for 15 sec., 58°C (BS) and 65C (CD) for 20 sec., and 72°C for 30 sec; followed with 10 min at 72°C. PCR products were seperated by electrophoresis on 2% agarose gels. Primers and PCR product fragments for BS, ATP8 and CD are listed in table.

Table Primer sequences and PCR products of the BS, ATP8 and CD

Gene names	Primer sequence	Fragment size	Literature
BS	F:5' GCTCAAGTAGTTAGTTGCTCCACTG3'	409 bp	Li, Y., et al., 2016
	R: 5' ATAAATAAATAAAGCAGGATGCTGAAA3'		
ATP8	F-W: 5' TAAGTTAGAGATTGAGAGCC3'	269 bp	
	R-W: 5' GATAAGGGTTACGAGAGGGA3'		
CD	Forward-W: 5'GGTGACCATCCTCTCTCTCTGC3'	436 bp	Menzi, F., et al., 2016
	Reverse: 5'AGTGGAACCCAGCTCCATTA3'		
	Forward-M: 5'CACCTTCCGCTATTCGAGAG3'	249 bp	

3 Results

In the study, a PCR technique was used to determine BS and CD carrier animals in Eskişehir population. PCR products were loaded onto a 2% agarose gel to detect BS in cattle. Li et al. (2016) proposed the use of the ATP8 gene as a positive control for PCR accuracy. The PCR results indicated the presence of 269 bp in all healthy and affected cattle with the BS genetic defect. Normal animals produced a single 269 bp fragment, while BS carriers produced 2 fragments of 269 and 409 bp (Fig 1). The electrophoresis band pattern revealed the presence of 2 heterozygous individuals for the BS among the studied cattle.

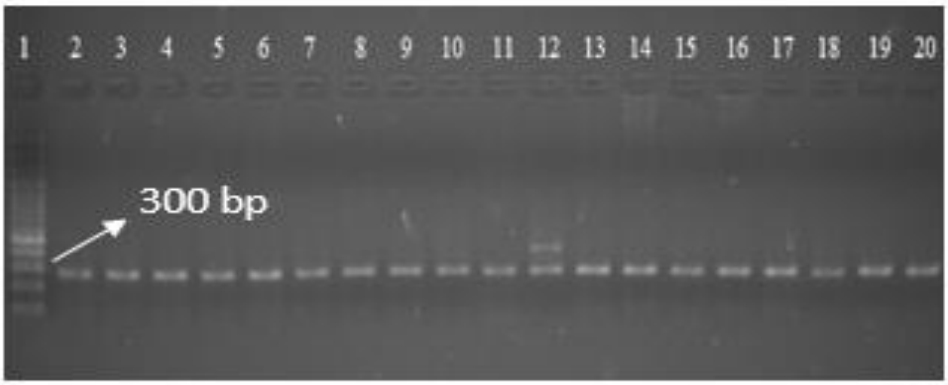

Fig 1. Electrophoretic band pattern for BS (M: 100 bp ladder; Fermentas® GeneRuler SMO241)

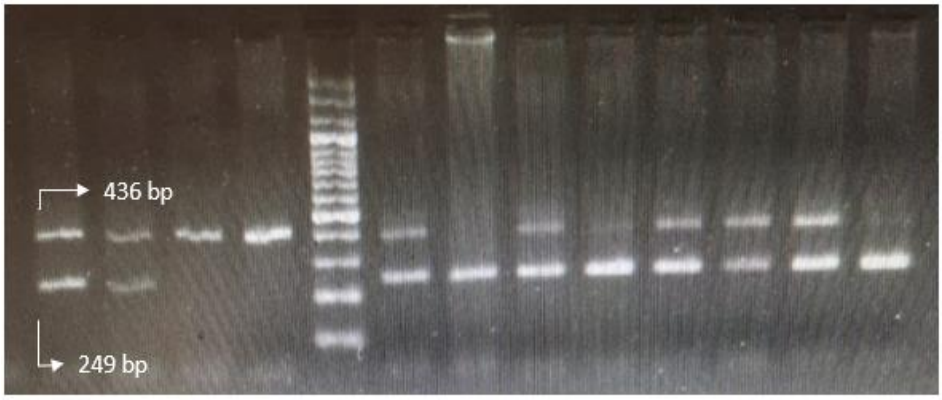

Fig 2. Electrophoretic band pattern for CD (L: 100 bp ladder; Fermentas® GeneRuler SMO241)

Menzi et al. (2016) developed and validated a PCR test using three primers to amplify 249 bp in healthy cattle, while 409 bp in CD-affected animals. CD carriers produced 2 fragments of 249 and 436 bp (Fig 2). During the visualization process, we identified 11 heterozygous individuals with CD among the studied cattle.

According to PCR studies carried out in Eskişehir, it was found that two out of the 112 Holstein cattle were affected by BS. Additionally, the deficiency allele for CD was present in eleven of them. The estimated frequency of the mutant and normal allele in CD and BS was 0.0491 and 0.0089, 0.9509 and 0.9911, respectively.

4 Conclusion

Predicting genetic disorders in animal husbandry and ensuring population health through controlled breeding are vital concerns. Identifying heterozygous animals is crucial for managing genetic diseases. Pre-breeding examination is necessary for cattle breeding to minimize risks. Molecular methods can be used to detect genetic diseases in animal populations. This approach will preserve the health of the future population and prevent any adverse impact on yield.

After the confirmed cases in Turkiye (Meydan et al., 2023), the cattle population in Eskişehir underwent a special examination for BS and CD genetic diseases, which resulted in the identification of the diseases.

The result of the study was determined that 2 and 11 Holstein cattle had the BS and CD mutant alleles, respectively, in the Eskişehir cattle population. Breeding selection should focus on reducing the frequency of genetic diseases in future populations through careful data analysis

Knowing the frequencies of these two genetic diseases that directly affect the yield in the population can identify the sires in the future population. This will prevent a direct decrease in yield by providing genetic disease control.

References

Agerholm JS (2007) Inherited disorders in Danish cattle, APMIS 115:1-76

Agerholm JS, McEvoy F, Arnbjerg J (2006) Brachyspina syndrome in a Holstein calf. J Vet Diagn Invest 18:418-422

Agerholm JS, Peperkamp K (2007) Familial occurrence of Danish and Dutch cases of the bovine brachyspina syndrome. BMC Vet Res 3:8

Agerholm JS, DeLay J, Hicks B, Fredholm M (2010) First confirmed case of the bovine brachyspina syndrome in Canada. Can Vet J 51:1349-1350

Bedir Dibıc K (2021) Türkiye'de Yetiştirilen Yerli Sığır ve Siyah Alaca Sığır Irklarında Brachyspina Sendromu ve Kolesterol Eksikliği Genetik Kusurlarının Belirlenmesi. Akdeniz Üniversitesi Fen Bilimleri Ensitüsü Tarımsal Biyoteknoloji Antalya

Buck BC, Ulrich R, Wöhlke A, Kuiper H, Baumgärtner W. (2010) Vertebral and multiple organ malformations in a black and white German Holstein calf. Berliner Und Münchener Tierärztliche Wochenschrift 123:251-255

Charlier C, Agerholm JS, Coppieters W., et al. (2012) A deletion in bovine *FANCI* gene compromises fertility by causing fetal death and brachyspine, PLoS ONE 7(8)

Chao CH, Chen YM, Lee KH (2020) Genotype screening of bovine brachyspina in Taiwan Holstein cows. Am J Anim Vet Sci 15(3):206-210

Kaminski S, Rusc A (2016) Cholesterol deficiency-new genetic defect transtmitted to Polish Holstein-Fresian cattle. Pol J Vet Sci 19(4):885-887

Kipp S, Segelke D, Reinhardt F, Reents R, Schierenbeck S, Wurmser C, Pausch H, Fries R, Thaller G, Tetens J, Pott J (2015) A new Holstein haplotype affecting calf survival. Interbull Bulletin p.49

Li Y, Zhai L, Fang L, Zhang S, Liu L, Zhu Y, Xue J, Xiaoqing L, Qiao L, Sun D (2016) A novel multiplex polymerase chain reaction method for the identification of brachyspina syndrome carriers in Chinese Holstein cattle. J Vet Sci Med Diagn 5(3)

Meydan H, Bedir Dibıc K, Vural O, Yıldız, M.A, Agerholm J (2023) Prevalence of carriers of cholesterol deficiency-associated APOB mutation in some native, Holstein and Simmental cattle breeds in Turkiye. Turk J Vet Anim Sci 47(6):584-587

Menzi F, Besuchet-Schmutz N, Fragnière M, Hofstetter S, Jagannathan V, Mock T, Raemy A, Studer E, Mehinagic K, Regenscheit N, Meylan M (2016) A transposable element insertion in *ABOP* causes cholesterol deficiency in Holstein cattle. Anim Genet 47(2):253-257

OMIA (2023) https://www.omia.org/OMIA001965/9913/ Accessed: 02/05/2023

Rusc A, Kaminski S (2015) Detection of brachyspina carriers within Polish Holstein-Fresian bulls. Pol J Vet Sci 18(2):453-454

Schütz E, Wehrhahn C, Wanjek M, Bortfeld R, Wemheuer WE, Beck J, Brenig B (2016) The Holstein Friesian lethal haplotype 5 (HH5) results from a complete deletion of TBF1M and cholesterol deficiency (CDH) from an ERV-(LTR) insertion into the coding region of APOB. PLoS ONE 11(4) :e0154602.

Testoni S, Diana A, Olzi E, Gentile A (2008) Brachyspina syndrome in two Holstein calves. Vet J 177(1):144-146

RESEARCH ARTICLE
Bull Biotechnol (2024) 5(1):11-18
https://doi.org/10.51539/biotech.1423000 Journal homepage: www.dergipark.org.tr/biotech

Bulletin of Biotechnology

Investigation of bioactive peptides from *Scolymus hispanicus* by using *in silico* methods

Levent Cavas[*1], Sema Dogmaz[2], Cagin Kandemir Cavas[3]

[*1]*Dokuz Eylül University, Faculty of Science, Department of Chemistry (Biochemistry Division), Kaynaklar Campus, 35390, İzmir, Türkiye*
[2]*Dokuz Eylül University, The Graduate School of Natural and Applied Sciences, Department of Biotechnology, Kaynaklar Campus, 35390, İzmir, Türkiye*
[3]*Dokuz Eylül University, Faculty of Science, Department of Computer Science, Kaynaklar Campus, 35390, İzmir, Türkiye*

*Corresponding author : levent.cavas@deu.edu.tr
Orcid No: https://orcid.org/0000-0003-2136-6928

Received : 20/01/2024
Accepted : 02/04/2024

To Cite: Cavas L, Dogmaz S, Kandemir Cavas C (2024) Investigation of bioactive peptides from Scolymus hispanicus by using *in silico* methods. Bull Biotechnol 5(1):11-18 https://doi.org/10.51539/biotech.1423000

Abstract: Due to increases in the soil pollution related to agricultural areas, the interests on the wild edible greens have been increasing nowadays. *Scolymus hispanicus* (=Golden thistle) is a wild edible plant which is widely and naturally spread in Türkiye. An *in silico*-based bioinformatics approach has been proposed for the evaluation of bioactive peptides from this species. *In silico* digestion and also bioactive peptides of RubisCO from *S.hispanicus* were studied by using BIOPEP-UWM. Protparam and Clustal Omega were also used to determine physicochemical parameters and sequence similarity, respectively. The A_E values related to angiotensin converting enzyme and dipeptidyl peptidase-IV were 0.0847 and 0.1059 after *in silico* pepsin digestion (pH>2), respectively. While the antioxidant property obtained after pepsin (pH>2) digestion was found to be 0.0127, the value of 0.042 was obtained for ficin on this parameter. BIOPEP-UWM also exhibit important properties related to the bioactivities of the peptides such as antioxidant, dipeptidyl peptidase-IV and angiotensin converting enzyme inhibitions. From the results, it could be said that *S. hispanicus* has very important bioactive peptides which could be evaluated in the production of functional foods. Moreover, isolated bioactive peptides and also secondary metabolites can also be utilized in pharmaceutical industry. Further *in vitro* and *in vivo* studies are strongly recommended on *S. hispanicus*.

Keywords: antioxidant; bioactive peptides; bioinformatics; *Scolymus hispanicus*; Golden thistle; functional foods

1 Introduction

Bioinformatics tools provide important contributions to understanding of biological functions in living organisms in various levels. Due to the big data related to protein and DNA sequences in various database, fast, robust and unbiased computational tools are necessary to explain structures in life sciences (Baxevanis et al. 2020). It is frequently observed in the literature that protein and DNA sequences evaluated in terms of bioinformatics are converted into numerical values and evaluated through computer-based algorithms (Kandemir-Cavas, 2023; Negi et al. 2023; Iqbal and Kumar, 2023).

Biopeptides can be determined as short chains of amino acids with diverse biological functions, including roles as signaling molecules, hormones, and antimicrobial agents. Bioinformatics also plays a crucial role in the analysis of biopeptides, providing valuable tools and methods to find out the complex information embedded in peptide sequences. It is of great importance to obtain biopeptides in their structures in order to evaluate agricultural products (Du et al. 2023). There are bioinformatics tools used to identify, characterize, detail and produce the bioactive mechanisms of bioactive peptides belonging to proteins that are very popular in the food and cosmetic industries today (Nuñez et al. 2020).

Wild food plants form an important part of many people's diets in a variety of local dishes (Guarrera and Savo, 2016). Golden thistle (*Scolymus hispanicus* L.), belongs to the Asteraceae family (Sergio, 2023). *S. hispanicus* is a thorny perennial herbaceous plant. This wild plant can be existed in wasteland, along the road, weedy areas and roadside ditches (Sergio, 2023, Polo et al. 2009). It is used as food in the Mediterranean countries such as Turkey, Spain, Portugal,

Morocco and Greece (Polo et al. 2009). Southern European nations are particularly interested in it due to its nutritional value and health benefits (Paschoalinotto, 2023). Young leaves, midribs, and root bark are all regarded as vegetables. Golden thistle is consumed with olive oil and meat, as well as in the form of tea (Figure 1).

Fig. 1 *Scolymus hispanicus* in Dokuz Eylül University Tınaztepe Campus, İzmir, Türkiye.

The essential oil of *S. hispanicus* included 15 constituents. Heneicosan (19.4%), acetone with hexahydrofarnel (17.0%), and phytol (17.0%) are the major chemicals. The most common were saturated n-alkane differentiation (35.2%), oxygenated sesquiterpenes (25.6%), and diterpenes (17%) (Servi, 2019). In its chemical analysis, high α-tocopherol content (2.79 ± 0.07 mg/100 g) in flowers, high gallic acid content (187.01 ± 10.19 mg/kg) in leaves and 3 flavonoids and 13 phenolic acids were identified (Marmouzi et al. 2017). This wild herb has hypoglycemic, antioxidant and anti-inflammatory properties (Berdja et al. 2021). Wild plants have been used for medical purposes since ancient times. Today, usage of wild edible plants has been gaining popularity as a healthful resource (Altiner and Sahan, 2016). In addition to its food properties, golden thistle also shows medicinal properties. The effect of the medicine called "Lityazol Cemil" on the kidney and bladder has been proven in clinical studies (Karik, 2019). Coşkun et al. (2021) investigated the effect of the extract obtained from the root of this plant in healing kidney stones, also known as calcium oxalate nephrolithiasis. Experimental results revealed the healing effect of the extract. Berdja et al. (2021) showed that studies showed that inclusion of *S. hispanicus* in a diet program or use as a nutritional supplement prevents metabolic damage by creating a hypoglycemic and hypolipidemic impact. It decreases oxidative stress, inflammation, and lipid buildup to improve glucose tolerance, hyperlipidemia, and hepatic steatosis (Berdja et al. 2021). Marmouzi et al. 2017 showed that the antioxidant and antidiabetic activities of the plant are through the inhibition of α-glucosidase and α-amylase. Components isolated from *S. hispanicus* inhibited NF-κB p65 expression in PHA-stimulated human PBMCs and subsequently showed anti-inflammatory properties in vitro as a result of reducing inflammatory cytokines (Kandil et al. 2020). *S. hispanicus* extract has a cytotoxic effect on Caco-2 cell growth, suggesting that it may have protective effects against colon cancer (Ahmad, 2017). Proteins in foods support health with their physiochemical roles as well as serving as nutrients (Daliri et al. 2017). Bioactive peptides are obtained from animal or plant-based sources (Cavas and Bilgin, 2021). Food-derived peptides display a number of biological functions in addition to their nutritional benefits, with effects such as antioxidative, hypoglycemic, hypocholesterolemic and antimicrobial (Nasri, 2017). Typically, bioactive peptides have 2 - 20 amino acid residues (Fan et al. 2014). Inhibition of the enzymes such as angiotensin converting enzyme (ACE) (EC 3.4.15.1) and dipeptidyl peptidase IV (DPP-IV) (EC 3.4.14.5) via bioactive peptides provides information about the function of biopeptides (Iwaniak et al. 2020). Bioactive peptides from foods are safe, effective, cost-effective, and bioavailable, leading to their investigation (Duffuler et al. 2022). This study reports, for the first time, the results from *in silico* tools related to the ribulose-1,5-bisphosphate carboxylase/oxygenase (RubisCO) bioactive peptides of the golden thistle plant. Additionally, the aim of the study was to estimate the functional food potential of the bioactive peptides from *S.hispanicus*.

2 Materials and Method

The proteins were searched on Uniprot.org using the term "*Scolymus hispanicus*" (The UniProt Consortium, 2019) and then the sequence of RubisCO from *S.hispanicus* was retrieved. The uniprot ID of RubisCO from *S.hispanicus* is G0WZG7. The amino acid sequence of *S. hispanicus* protein was retrieved from Uniprot.org in FASTA format (Morgat et al. 2019).

The physical and chemical characteristics of the protein from *S. hispanicus* were identified using the ProtParam tool (Gasteiger et al. 2005). This tool was used to calculate molecular weight, number, net charge, amino acid percentage and theoretical pI value and instability index.

Amino acid or nucleotide sequence multiple sequence alignments are quickly and accurately provided using Clustal Omega tool (Sievers and Higgins, 2014). The sequences of RubisCO proteins of the plants were compared using the Clustal Omega tool.

Bioactive peptides reported in *S. hispanicus* were searched using the BIOPEP-UWM tool (Minkiewicz et al. 2019). To analyze the values of the quantitative parameters of BIOPEP-UWM for bioactive peptides, the following procedures were performed. The enzymes used in the research as follow: chymotrypsine (EC3.4.21.1), trypsin (EC3.4.21.4), pepsin (pH 1.3) (EC3.4.23.1), proteinase K (EC3.4.21.64), pancreatic elastase (EC3.4.21.36), prolyl oligopeptidase (EC3.4.21.26), V-8 protease (Glutamyl endopeptidase; pH=4 (EC3.4.21.19), thermolysin (EC3.4.24.27), chymotrypsin C

(EC3.4.21.2), plasmin (EC3.4.21.7), cathepsin (EC3.4.21.20), clostripain (EC3.4.22.8), chymase (EC3.4.21.39), papain (EC3.4.22.2), ficin (EC3.4.22.3), leukocyte elastase (EC3.4.21.37), metridin (EC3.4.21.3), pancreatic elastase II (EC3.4.21.71), stem bromelain (EC3.4.22.32), glutamyl endopeptidase II (EC3.4.21.82), oligopeptidase B (EC3.4.21.83), calpain 2 (EC3.4.22.53), glycyl endopeptidase (EC3.4.22.25), oligopeptidase F, proteinase P1 (lactocepin) (EC3.4.21.96), Xaa-Pro dipeptidase (EC3.4.13.9), pepsin (pH>2) (EC3.4.23.1), coccolysin (EC3.4.24.30), subtilisin (EC3.4.21.62), chymosin (EC3.4.23.4), ginger protease (zingipain) (EC3.4.22.67) and V-8 protease (glutamyl endopeptidase); pH=7.8 (EC3.4.21.19).

3 Results and Discussion

RubisCO of *S.hispanicus* peptides was obtained by *in silico* proteolytic digestion with BIOPEP tools. The results were also compared with the common plants such as *Anethum graveolens* and *Eruca sativa*. The results from BIOPEP parameters (B_E, A_E, W, DH_t and V) were shown in Tables 1-5.

The theoretical degree of hydrolysis (DHt), indicates the enzyme's efficiency in producing peptides from *S. hispanicus*. The highest DHt values were obtained to be 71.9149, 52.3404 and 42.9787 by using pepsin (pH>2), pancreatic elastase and ficin enzymes, respectively. Although the highest values were observed in pepsin, pancreatic elastase and ficin, the minimum values were found when chymosin, ginger protease (zingipain) and thrombin were used. W is a measure of how frequently an enzyme releases fragments with a specific level of activity. B_E refers to the activity of potentially released fragments by the proteolytic enzymes. According to Gasteiger et al. (2005), V denotes the relative activity of fragments with particular activity produced by the selected enzymes. The frequency with which the chosen enzyme releases fragments with a particular activity is known as the parameter A_E (Minkiewicz et al. 2019). Using the BIOPEP-UWM tool, the functions of biologically active peptides such as antioxidant peptides, ACE inhibitor, dipeptidyl peptidase III, DPP-IV inhibitor can be determined *in silico* tools (Iwaniak et al. 2015).

Biological activities of *S. hispanicus*, *E. sativa* and *A. graveolens* biopeptides are shown in Tables 1-5. As a result of *in silico* analysis, regulating, activating ubiquitin-mediated proteolysis and stimulating activity were observed in biopeptides obtained from these foods. Anticoagulant peptides have different efficacy in preventing thrombosis. The incidence of cardiovascular disease can be prevented and decreased with the help of antithrombotic-rich diets (Cheng et al. 2019). The antiamnestic effect of some bioactive peptides may play an important role in the treatment and prevention of mental disorders (Garmidolova et al. 2022). DPP-III is involved in a number of physiological and pathological processes, including defense from oxidative stress, apoptosis, as inflammation, besides to its role in the protein cycle's final stages (Tomi et al. 2023). Alpha glucosidase inhibitors delay the absorption of glucose by reducing the digestion of carbohydrates and lower blood glucose levels without insulin being secreted (Abbasi et al. 2022).

Table 1 BIOPEP Bioactivity parameters related to enzymatic digestion (ficin (EC 3.4.22.3)) of *Scolymus hispanicus*. (NAN: not a number)

DH_t [% 42.9787]					
No	**Activity**	**A_E**	**W**	**B_E**	**V**
1	regulating	0.0042	0.1654	0	NAN
2	ACE inhibitor	0.0678	0.1111	0.0018	0.0511
3	antioxidative	0.0042	0.0367	0	0
4	dipeptidyl peptidase IV inhibitor	0.0763	0.1233	0.0001	0.4036
5	HMG-CoA reductase inhibitor	0.0042	1.0000	0	NAN
6	renin inhibitor	0.0042	0.1239	1.37E-6	1
7	dipeptidyl peptidase III inhibitor	0.0085	0.0669	0	NAN

Table 2 BIOPEP Bioactivity parameters related to enzymatic digestion (pancreatic elastase (EC 3.4.21.36)) of *Scolymus hispanicus*. (NAN: not a number)

DH_t [%52.3404]					
No	**Activity**	**A_E**	**W**	**B_E**	**V**
1	Regulating	0.0042	0.1654	0	NAN
2	dipeptidyl peptidase IV inhibitor	0.0975	0.1576	1.83E-5	0.0605
3	ACE inhibitor	0.0678	0.1127	0.0008	0.022
4	Antithrombotic	0.0042	0.3307	0	NAN
5	Antiamnestic	0.0042	0.3307	0	NAN
6	activating ubiquitin-mediated proteolysis	0.0085	0.6693	0	NAN
7	dipeptidyl peptidase III inhibitor	0.0042	0.0330	0	NAN
8	alpha-glucosidase inhibitor	0.0042	0.0708	2.49E-7	0.0013
9	anti inflammatory	0.0042	0.4941	0	NAN

The peptides that inhibit DPP-IV are therapeutic for diabetes type 2. Anti-diabetic peptide controls the levels of glucose in the blood and stops incretins from degrading by inhibiting DPP-IV (Lu et al. 2022). DPP-IV inhibition related bioactive peptides obtained from *S.hispanicus* RubisCO by cleavage with pancreatic elastase is 0.0975 (Table 1), after digestion with ficin it was found as 0.0763 (Table 2). As a result of *in silico* digestion by pepsin, DPP-IV value was found to be 0.1059 (Table 3). When Pepsin (pH>2) (EC3.4.23.1) was used, the DPP-IV based A_E values of the biopeptides obtained from *E. sativa* and *A. graveolens* RubisCOs were found to be 0.0593 and 0.0750, respectively.

Table 3 BIOPEP Bioactivity parameters related to enzymatic digestion (pepsin (pH>2) (EC3.4.23.1)) of *Scolymus hispanicus*. (NAN: not a number)

DH_t [% 71.9149]					
No	**Activity**	**A_E**	**W**	**B_E**	**V**
1	regulating	0.0042	0.1654	0	NAN
2	dipeptidyl peptidase IV inhibitor	0.1059	0.1712	5.92E-5	0.1962
3	ACE inhibitor	0.0847	0.1388	0.0045	0.1286
4	antithrombotic	0.0042	0.3307	0	NAN
5	antiamnestic	0.0042	0.3307	0	NAN
6	activating ubiquitin-mediated proteolysis	0.0085	0.6693	0	NAN
7	antioxidative	0.0127	0.1110	0	0
8	stimulating	0.0042	0.1654	0	NAN
9	dipeptidyl peptidase III inhibitor	0.0169	0.1330	0	NAN
10	alpha-glucosidase inhibitor	0.0085	0.1433	3.60E-7	0.0019
11	anti inflammatory	0.0042	0.4941	0	NAN

Iram et al. 2022 used an *in silico* method to analyze bioactive peptides for the breakdown of sheep protein from milk via digestive enzymes. DPP-IV inhibitory peptides observed in BIOPEP-UWM, including casein, s1 casein, s2 casein, lactalbumin and lactoglobulin had A_E values of 0.4504, 0.4158, 0.4304, 0.4929, and 0.4611, respectively. The bioactive peptide capacity of tomato grain, an advantageous industrial waste, was researched by Kartal et al. in 2020. The greatest A values for possible DPP-IV inhibitory effects came from 11S globulin, profilin, and SNF4 and were 0.6819, 0.6794, and 0.6676, respectively. Portuguese oyster (*Crassostrea angulata*) peptides were studied by Gomez et al. 2019, to examine their potential bioactivities *in vitro* as well as *in silico*. Among the 9 enzymes used, theoretical DPP-IV activity was found to be high in pepsin (pH > 2), papain and root bromelain. The bioactive peptide numbers of these three enzymes were found to be 333, 290 and 280, respectively.

Table 4 BIOPEP Bioactivity parameters related to enzymatic digestion (pepsin (pH>2) (EC3.4.23.1)) of *Eruca sativa.* (NAN: not a number)

DH_t [%47.0270]					
No	**Activity**	**A_E**	**W**	**B_E**	**V**
1	regulating	0.0054	0.4000	0	NAN
2	dipeptidyl peptidase IV inhibitor	0.0593	0.1583	3.87E-5	0.2014
3	ACE inhibitor	0.0404	0.1135	0.0021	0.0872
4	antithrombotic	0.0027	0.3333	0	NAN
5	antiamnestic	0.0027	0.3333	0	NAN
6	activating ubiquitin-mediated proteolysis	0.0027	0.3333	0	NAN
7	antioxidative	0.0054	0.0801	0	0
8	stimulating	0.0027	0.1667	0	NAN
9	dipeptidyl peptidase III inhibitor	0.0108	0.1484	0	NAN
10	alpha-glucosidase inhibitor	0.0054	0.1337	2.29E-7	0.0018

The A_E value of the ACE inhibitor of bioactive peptides obtained from RubisCO of *S. hispanicus* was 0.0678 when pancreatic elastase and ficin were used, while it was found as 0.0847 when pepsin was used. The A_E value of the ACE inhibitor of bioactive peptides obtained from RubisCO of *E. sativa* shown in Table 4 was 0.0404 for pepsin (pH>2) (EC3.4.23.1), while it was 0.0500 for *A. graveolens* in Table 5. It is used to reduce blood pressure in people with hypertension because it eliminates the vasodilator bradykinin and catalyzes the transformation of the angiotensin I-converting enzyme (ACE) into the strong vasoconstrictor angiotensin II (Iwaniak et al. 2015; Karami et al. 2019).

Panjaitan et al. (2018) demonstrated that protein bioactivities from giant grouper eggs using the BIOPEP-UWM database. The values obtained using BIOPEP-UWM for amino acid sequence, vitellogenin ACE inhibitor, apolipoprotein A-1 precursor, and *Epinephelus coioides* activity were 0.408, 0.388, and 0.334, respectively.. Utilizing the BIOPEP-UWM database, Arámburo-Gálvez et al. (2022) assessed legume and provicillin protein sequences for forecasting of ACE-I inhibitory peptides. ACE-I inhibitory peptides of legume, provicilin and papain have been identified to have A_E values of 0.0605-0.0442 and 0.0323-0.0287, respectively. Buffalo milk proteins' ability to release both familiar and new bioactive peptides was studied by Gu et al. in 2023. The ACE inhibitory values of α lactalbumin, β lactoglobulin, α s1 casein, α s2 casein, β casein and K casein were 0.394, 0.528, 0.556, 0.405, 0.679 and 0.447, respectively.

Table 5 BIOPEP Bioactivity parameters related to enzymatic digestion (pepsin (pH>2) (EC3.4.23.1)) of *Anethum graveolens.* (NAN: not a number)

DH_t [%48.7465]					
No	**Activity**	**A_E**	**W**	**B_E**	**V**
1	regulating	0.0056	0.4029	0	NAN
2	dipeptidyl peptidase IV inhibitor	0.0750	0.1929	7.96E-5	0.3502
3	ACE inhibitor	0.0500	0.1333	0.0024	0.1026
4	antithrombotic	0.0028	0.5000	0	NAN
5	antiamnestic	0.0028	0.5000	0	NAN
6	activating ubiquitin-mediated proteolysis	0.0056	0.6747	0	NAN
7	antioxidative	0.0056	0.0776	0	0
8	stimulating	0.0028	0.1677	0	NAN
9	dipeptidyl peptidase III inhibitor	0.0111	0.1377	0	NAN
10	alpha-glucosidase inhibitor	0.0056	0.1440	2.36E-7	0.0019

Antioxidant-active peptidesregulate oxidative processes within the body of humans. Numerous degenerative diseases can start or advance because of free radicals. Illnesses and oxidative stress are closely related. To lessen oxidative stress, many antioxidants have been obtained and produced from natural sources (Sarmadi and Ismail, 2010). Antioxidative properties of biopeptides from RubisCO of *S. hispanicus* when pepsin and ficin used were also studied in the present study. The A_E values were 0.0127 and 0.0042, respectively. As opposed to that, no antioxidative property was observed when pancreatic elastase was used. When the antioxidative properties of bioactive peptides obtained from RubisCO of *E. sativa* showed in Table 4 were examined, the A_E value was 0.0054 for pepsin (pH>2) (EC3.4.23.1), while it was 0.0056 for *A. graveolens* (Table 5). Antioxidant peptides are also of great importance in foods, as they can limit oxidative damage and affect nutritive and beneficial. This may lessen food oxidative deterioration. Biopeptides, when taken in the diet as antioxidants, protect body cells from oxidation (Leo et al. 2016). Panjaitan et al. 2022 investigated the antioxidant and Angiotensin-I converting enzyme (ACE-I) inhibitory effect of steam-cooked mackerel (*Scomber australasicus*) juice utilizing both *in silico* and *in vitro* analysis methods. The antioxidant activity was hydrolyzed utilizing proteases papain, pepsin, proteinase k, alkalase, bromelain and thermolysin 36, 23, 29, 20, 27, 41, 25, 16 and 22, respectively. Millan et al. 2022 studied antioxidant and antihypertensive activities as a result of hydrolysis with protease were investigated in cold *Lysobacter sp*. The A_E values were found to be 0.0169, 0.0103 and 0.0033, respectively, when β-lactoglobulin, lactoferrin, and serum albumin were studied. Cavas et al. 2020 studied the bioactive content of *Lagocephalus sceleratus*, known as a poisonous fish due to its toxins, were evaluated using an *in silico*-based biotechnological approach. The A_E value of the antioxidant activity of L. sceleratus protein cytochrome c oxidase subunit 1 was found to be 0.0108 using pepsin (pH = 1.3) enzymes.

The functions of the peptides depend on their specific amino acid composition and sequence, as well as some hydrophobic amino acids that bring about the antioxidant function of the biopeptides (Wen et al. 2020). The percentage of the essential amino acids was determined to be 40.6% in the *S. hispanicus* RuBisCO (Table 6). It was found that glycine (9.6%), alanine (8.7%), tyrosine (8.3%), and leucine (8.3%) made up the majority of RuBisCO. The content of proline amino acid was determined to be 6.1%. Table 7 lists the net charges of the proteins from *S. hispanicus*, *E. sativa*, and *A. graveolens* RubisCOs were found with the values of -2, -4, and -3, respectively. The stability index for the proteins, which were found to be 28.76, 33.34, and 28.41, respectively, indicated that the proteins were stable.

Using *in vitro* and *in silico* techniques, the ability of Gouda cheese with a modified casein content to inhibit ACE- and DPP-IV was investigated by Iwaniak et al (2021). The commonest amino acids found encompass all genetic variants of S1 according to the ProtParam study were 0.6-12.1% Glutamic acid, 7.5-10.3% Leucine, 7.9-9.1% Proline, 7.5-8.6% Serine, and 7.0-7.5% Lysine. Ağırbaşlı and Cavas (2017) studied bioactive peptides of 28 *Caulerpa spp.* using *in silico* methods. It was discovered that the range of total essential amino acids in *Caulerpa spp*'s RuBisCO findings was between 45 and 47%. It was found that 10.2-11.5% glycine, 8.6-10.9% alanine and 8.9-9.8% leucine made up the majority of RuBisCO. Cavas and Abeska 2020 examined the allergenicity of the endochitinase class 1 (Pers a 1) protein found in avocados using bioinformatics techniques in their study. According to Prot param results, the most numerous amino acids included in endochitinase of the allergen protein *Persea americana* plant are glycine (4.3%), alanine (11%) and serine (7.1%).

Figure 2 displays the level of similarity between *S. hispanicus, E. sativa*, and *A. graveolens* identified through the Clustal Omega database. An asterisk (*), a colon (:), and a period (.) are used in the cluster omega results to denote conserved residues, comparable characteristics, and barely similar traits, respectively. The study contrasts the RubisCo bioactive peptide contents of *S. hispanicus* with those of *A. graveolens*, and *E. sativa*. One may say that RubisCO of these species are remarkably similar to one another. As a result of different enzymatic hydrolysis, the highest DHt value was found in *S. hispanicus*. DHt (%) values obtained as a result of hydrolysis of *E. sativa* and *A. graveolens* with pepsin were found to be 47.0270 and 48.7465, respectively. The AE value of *S. hispanicus* due to ACE inhibition is significantly higher than the other plants examined. Since ACE, antioxidant and DDT-IV values of *E. sativa*, and *A. graveolens* are very close to each other, *S. hispanicus* can be used as an alternative source.

Table 6 Number and percentage of amino acids found in *Scolymus hispanicus.*

Amino acid composition:	#	%
Ala (A)	20	8.70%
Arg (R)	13	5.70%
Asn (N)	8	3.50%
Asp (D)	12	5.20%
Cys (C)	4	1.70%
Gln (Q)	6	2.60%
Glu (E)	17	7.40%
Gly (G)	22	9.60%
His (H)	2	0.90%
Ile (I)	9	3.90%
Leu (L)	19	8.30%
Lys (K)	14	6.10%
Met (M)	2	0.90%
Phe (F)	11	4.80%
Pro (P)	14	6.10%
Ser (S)	7	3.00%
Thr (T)	19	8.30%
Trp (W)	3	1.30%
Tyr (Y)	14	6.10%
Val (V)	14	6.10%
Pyl (O)	0	0.00%
Sec (U)	0	0.00%
(B)	0	0.00%
(Z)	0	0.00%
(X)	0	0.00%

Table 7 Protein parameters of *Scolymus hispanicus*, *Eruca sativa*, *Anethum graveolens* found in RubisCO.

Species	#aa	MW (Kda)	Theoretical pI	Negatively Charged Residues (Asp+Glu)	Positively Charged Residues (Arg+Lys)	Net Charge	Instability Index
Scolymus hispanicus	230	25635.02	5.84	29	27	-2	28.76
Eruca sativa	215	24105.25	5.36	28	24	-4	33.34
Anethum graveolens	215	24083.25	5.38	28	25	-3	28.41

Fig. 2 Multiple sequence analysis of RubisCOs from *Scolymus hispanicus*, *Eruca sativa* and *Anethum graveolens*.

.

5 Conclusion

Functional nutrition is of great importance in preventing and controlling autoimmune diseases that develop due to nutrition. From this point, it could be said that bioactive peptides from various plant sources are of great importance for development of functional foods (Tu el al. 2018; Peredo-Lovillo et al. 2022).

Determining the biopeptides in the structure of proteins in experimental environments is both time consuming and costly. Nowadays, accurate, precise results can be obtained in a short time by using bioinformatics tools for biopeptide analysis (Dang et al. 2022; Agyei et al. 2019).

Due to soil contamination and also interest on wild edible plants, importance of *S. hispanicus* is being increased in Türkiye. The price of *S.hispanicus* is about 5 Euro/kg in local bazaars. In order to assess the bioactive peptides of the wild *S. hispanicus* plant, which grows in wastelands, and untamed areas, an *in silico*-based biotechnological technique has been suggested in this study. The present article reveals that *S. hispanicus* contains important bioactive peptides. In the nations where the plant is produced, these peptides should be isolated and utilized. In the pharmaceutical industry, isolated bioactive peptides and secondary metabolites can also be employed. The results revealed from the study clearly show that the bioactive potential of *S. hispanicus* peptides should be effectively utilised. The results of this study also support the plant's suitability as a functional food. Golden thistle bioactive peptides thus offer promise for the development of nutraceutical products. However, to see the full potential of the plant, further *in vitro* and *in vivo* experiments are recommended to validate *in silico* results.

Acknowledgements

SD is a Master of Science Student in Dokuz Eylül University, Department of Biotechnology (İzmir, Türkiye). This research did not receive any specific grant from funding agencies in the public, commercial, or not-for-profit sectors.

Authors' contributions:

The study's inception, design, data collecting, writing, original draft preparation, writing, review, and editing were all contributed by LC, SD and CKC.

Conflict of interest disclosure:

The authors declare no conflict of interest.

References

Abbasi S, Moslehishad M, Salami M. (2022) Antioxidant and alpha-glucosidase enzyme inhibitory properties of hydrolyzed protein and bioactive peptides of quinoa. Int J Biol Macromol 213, 602-609.

Agirbasli Z, Cavas L. (2017) *In silico* evaluation of bioactive peptides from the green algae *Caulerpa*. J Appl Phycol *29*, 1635-1646.

Agyei, D., Bambarandage, E., & Udenigwe, C. C. (2019). The role of bioinformatics in the discovery of bioactive peptides.

Ahmad B. (2017) Extraction of phytochemicals from *Scolymus hispanicus* and determination of potential health effects (Doctoral dissertation, Izmir Institute of Technology (Turkey)).

Altiner DD, Sahan, Y. (2016) A functional food additive: *Scolymus Hispanicus* L. Flour. Int J Food Eng 2(2), 124-27.

Arámburo-Gálvez JG, Arvizu-Flores AA, Cárdenas-Torres FI, Cabrera-Chávez F, Ramírez-Torres GI, Flores-Mendoza LK, Gastelum-Acosta PE, Figueroa-Salcido OG, Ontiveros N. (2022) Prediction of ACE-I inhibitory peptides derived from chickpea (*Cicer arietinum* L.): *in silico* assessments using simulated enzymatic hydrolysis, molecular docking and ADMET evaluation. Foods 11(11), 1576.

Baxevanis, A. D., Bader, G. D., & Wishart, D. S. (Eds.). (2020). Bioinformatics. John Wiley & Sons.

Berdja S, Boudarene L, Smail L, Neggazi S, Boumaza S, Sahraoui A, Haffaf EM, Kacimi G, Aouichat Bouguerra S. (2021) *Scolymus hispanicus* (Golden Thistle) Ameliorates Hepatic Steatosis and Metabolic Syndrome by Reducing Lipid Accumulation, Oxidative Stress, and Inflammation in Rats under Hyperfatty Diet. Evid Based Complementary Altern Med 2021, 1-14.

Çavaş L, Bilgin Y, Yilmaz-Abeşka Y. (2020) Can bioactive peptides of *Lagocephalus sceleratus* be evaluated in the functional food industry?. Biotech Studies 29(2), 77-84.

Çavaş L, Bilgin Y. (2021) Bioactivities from novel toxins of *Pterois volitans*: A Bioinformatics approach. Gazi Univ J Sci 8(4), 411-423.

Çavas L, Yilmaz-Abeska Y. (2023) Identification of Novel Endochitinase Class I Based Allergens. Asthma Allergy Immunol 21(1).

Cheng S, Tu M, Liu H, Zhao G, Du M. (2019) Food-derived antithrombotic peptides: Preparation, identification, and interactions with thrombin. Crit Rev Food Sci Nutr 59(sup1), S81-S95.

Daliri EBM, Oh DH, Lee BH. (2017) Bioactive peptides. Foods 6(5), 32.

Dang, C., Okagu, O., Sun, X., & Udenigwe, C. C. (2022). Bioinformatics analysis of adhesin-binding potential and ADME/Tox profile of anti-Helicobacter pylori peptides derived from wheat germ proteins. Heliyon, 8(6).

Du Z, Comer J, Li Y. (2023). Bioinformatics approaches to discovering food-derived bioactive peptides: Reviews and perspectives. TrAC Trends Anal Chem 117051.

Duffuler P, Bhullar KS, de Campos Zani SC, Wu J. (2022) Bioactive peptides: From basic research to clinical trials and commercialization. J Agric Food Chem 70(12), 3585-3595.

Fan X, Bai L, Zhu L, Yang L, Zhang X. (2014) Marine algae-derived bioactive peptides for human nutrition and health. J Agric Food Chem 62(38), 9211-9222.

Gasteiger E, Hoogland C, Gattiker A, Wilkins MR, Appel RD, Bairoch A. (2005) Protein identification and analysis tools on the ExPASy server. In The proteomics protocols handbook, 571-607. Humana press.

Garmidolova, A., Desseva, I., Mihaylova, D., Lante, A. (2022). Bioactive peptides from *lupinus spp.* seed proteins-state-of-the-art and perspectives. Appl Sci 12(8), 3766.

Gu Y, Li X, Qi X, Ma Y, Chan ECY. (2023) *In silico* identification of novel ACE and DPP-IV inhibitory peptides derived from buffalo milk proteins and evaluation of their inhibitory mechanisms. Amino Acids 55(2), 161-171.

Guarrera PM, Savo V. (2016) Wild food plants used in traditional vegetable mixtures in Italy. J Ethnopharmacol 185, 202-234.

Gomez HLR, Peralta JP, Tejano LA, Chang YW. (2019) *In silico* and in vitro assessment of portuguese oyster (*Crassostrea angulata*) proteins as precursor of bioactive peptides. Int J Mol Sci 20(20), 5191.

Iqbal N, Kumar P. (2023). From Data Science to Bioscience: Emerging era of bioinformatics applications, tools and challenges. Procedia Comp Sci 218, 1516-1528.

Iram D, Sansi MS, Zanab S, Vij S, Ashutosh, Meena S. (2022) *In silico* identification of antidiabetic and hypotensive potential bioactive peptides from the sheep milk proteins—a molecular docking study. J Food Biochem 46(11), e14137.

Iwaniak A, Minkiewicz P, Darewicz M, Protasiewicz M, Mogut D. (2015) Chemometrics and cheminformatics in the analysis of biologically active peptides from food sources. J Funct Foods 16, 334-351.

Iwaniak A, Minkiewicz P, Pliszka M, Mogut D, Darewicz M. (2020) Characteristics of biopeptides released *in silico* from collagens using quantitative parameters. Foods, 9(7), 965.

Iwaniak A, Mogut D, Minkiewicz P, Żulewska J, Darewicz M. (2021) Gouda cheese with modified content of β-casein as a source of peptides with ACE-and DPP-IV-inhibiting bioactivity: A study based on *in silico* and in vitro protocol. Int J Mol Sci 22(6), 2949.

Kamer Coşkun N, Coşkun A, Ertas B, Ahmad S, Ümit Özdöl M, Çankaya S, Çetinkol Y, Ozel Y, Elçioğlu, HK. (2022). Dose-dependent effect of *Scolymus hispanicus* L.(sevketibostan) on ethylene glycol-induced kidney stone disease in rats. Indian J Biochem Biophys 59(1), 7-13.

Kandemir-Cavas C, Pérez-Sanchez H, Mert-Ozupek N, Cavas L. (2019). In silico analysis of bioactive peptides in invasive sea grass Halophila stipulacea. Cells, 8(6), 557.

Kandil ZA, Esmat A, El-Din RS, Ezzat SM. (2020) Anti-inflammatory activity of the lipophilic metabolites from *Scolymus hispanicus* L. S Afr J Bot 131, 43-50.

Karami Z, Akbari-Adergani B. (2019) Bioactive food derived peptides: A review on correlation between structure of bioactive peptides and their functional properties. J Food Sci Technol 56, 535-547.

Karik U. (2019) The effect of different harvest dates on the yield and quality of the golden thistle (*Scolymus hispanicus* L.). Turkish J Field Crop 24(2), 230-236.

Kartal C, Kaplan Türköz B, Otles S. (2020) Prediction, identification and evaluation of bioactive peptides from tomato seed proteins using *in silico* approach. J Food Meas Charact 14(4), 1865-1883.

Leo EEM, Fernández JJA, Campos MRS. (2016) Biopeptides with antioxidant and anti-inflammatory potential in the prevention and treatment of diabesity disease. Biomed Pharmacother 83, 816-826.

Lu Z, Sun N, Dong L, Gao Y, Lin S. (2022) Production of bioactive peptides from sea cucumber and its potential health benefits: A comprehensive review. J Agric Food Chem 70(25), 7607-7625.

Marmouzi I, El Karbane M, El Hamdani M, Kharbach M, Naceiri Mrabti H, Alami R, Dahraoui S, El Jemli M, Ouzzif Z, Cherrah Y, Derraji S, Faouzi, MEA. (2017) Phytochemical and pharmacological variability in Golden Thistle functional parts: comparative study of roots, stems, leaves and flowers. Nat Prod Res 31(22), 2669-2674.

Millan GCL, Veras FF, Stincone P, Pailliè-Jiménez ME, Brandelli A. (2022) Biological activities of whey protein hydrolysate produced by protease from the Antarctic bacterium *Lysobacter sp.* A03. Biocatal Agric Biotechnol 43, 102415.

Minkiewicz P, Iwaniak A, Darewicz M. (2019) BIOPEPUWM database of bioactive peptides: Current opportunities. Int J Mol Sci 20(23), 5978.

Morgat A, Lombardot T, Coudert E, Axelsen K, Neto TB, Gehant S, Bansal P, Bolleman J, Gasteiger E, de Castro E, Baratin D, Pozzato M, Xenarios I, Poux S, Redaschi N, Bridge A, The UniProt Consortium. (2019) Enzyme annotation in UniProtKB using Rhea. Bioinformatics 36(6), 1896-1901.

Nasri M. (2017) Protein hydrolysates and biopeptides: Production, biological activities, and applications in foods and health benefits. A review. Adv Food Nutr Res 81, 109-159.

Negi S.S, Schein CH, Braun W. (2023). The updated Structural Database of Allergenic Proteins (SDAP 2.0) provides 3D models for allergens and incorporated bioinformatics tools. J Allergy Clin Immunol Glob 2(4), 100162.

Nuñez SM, Guzmán F, Valencia P, Almonacid S, Cárdenas C. (2020). Collagen as a source of bioactive peptides: A bioinformatics approach. Electron J Biotechnol 48, 101-108.

Panjaitan FCA, Gomez HLR, Chang YW. (2018) *In silico* analysis of bioactive peptides released from giant grouper (*Epinephelus lanceolatus*) roe proteins identified by proteomics approach. Molecules 23(11), 2910.

Panjaitan FCA, Chen TY, Ku HH, Chang YW. (2022) *In Silico* and In Vitro Analyses of Angiotensin-I Converting Enzyme Inhibitory and Antioxidant Activities of Enzymatic Protein Hydrolysates from Taiwan Mackerel (*Scomber australasicus*) Steaming Juice. Foods 11(12), 1785.

Paschoalinotto BH, Polyzos N, Compocholi M, Rouphael Y, Alexopoulos A, Dias MI, Barros L, Petropoulos SA. (2023) Domestication of Wild Edible Species: The Response of *Scolymus hispanicus* Plants to Different Fertigation Regimes. Horticulturae *9*(1), 103.

Peredo-Lovillo A, Hernández-Mendoza A, Vallejo-Cordoba B, Romero-Luna HE. (2022). Conventional and in silico approaches to select promising food-derived bioactive peptides: A review. Food Chem X, 13, 100183.

Polo S, Tardío J, Vélez-del-Burgo A, Molina M, Pardo-de-Santayana M. (2009) Knowledge, use and ecology of golden thistle (*Scolymus hispanicus* L.) in Central Spain. J Ethnobiol Ethnomedicine 5, 1-13.

Sarmadi BH, Ismail A. (2010) Antioxidative peptides from food proteins: A review. Peptides 31(10), 1949-1956.

Sergio L, Di Venere D, Gonnella M, D'Imperio M, Baruzzi F, Pinto L, Boari F, Cantore V, Candido V. (2023) Quality and Safety of Ready-to-Eat Golden Thistle (*Scolymus hispanicus L.*): A New Product for Traditional Italian Dishes. Plants *12*(8), 1622.

Servi H. (2019) Essential oil composition from aerial parts of *Scolymus hispanicus* L. A J Health Sci 1(2), 87-94.

Sievers F, Higgins DG. (2014) Clustal omega. Curr Protoc Bioinformatics *48*(1), 3-13.

The UniProt Consortium. (2019) UniProt: a worldwide hub of protein knowledge. Nucleic Acids Res 47, 506-515

Tomić, A., Karačić, Z., & Tomić, S. (2023). Influence of Mutations of Conserved Arginines on Neuropeptide Binding in the DPP III Active Site. Mol 28(4), 1976.

Tu M, Cheng S, Lu W, Du M. (2018). Advancement and prospects of bioinformatics analysis for studying bioactive peptides from food-derived protein: Sequence, structure, and functions. TrAC Trends Anal Chem 105, 7-17.

Wen C, Zhang J, Zhang H, Duan Y, Ma H. (2020) Plant protein-derived antioxidant peptides: Isolation, identification, mechanism of action and application in food systems: A review. Trends Food Sci Technol 105, 308-322.

RESEARCH ARTICLE
Bull Biotechnol (2024) 5(1):19-23
https://doi.org/10.51539/biotech.1476039 Journal homepage: www.dergipark.org.tr/biotech

Bulletin of Biotechnology

Three-dimensional reconstruction and morphometry of the mandible in New Zealand rabbits

Muhammet Lütfi Selçuk*

*[1]*Department of Physiotherapy and Rehabilitation, Faculty of Health Sciences, Karamanoglu Mehmetbey University, Karaman, Türkiye*

*Corresponding author : mlselcuk@hotmail.com
Orcid No: https://orcid.org/0000-0002-9915-3829

Received : 30/04/2024
Accepted : 14/06/2024

To Cite: Selçuk ML (2024) Three-dimensional reconstruction and morphometry of the mandible in New Zealand rabbits. Bull Biotechnol 5(1):19-23 https://doi.org/10.51539/biotech.1476039

Abstract: This study was conducted to create three-dimensional (3D) models of the lower jaw using computed tomography (CT) images of New Zealand rabbits and to reveal whether there are differences between genders. 12 New Zealand rabbits (6 female, 6 male) were used in the study. Computed tomography (CT) images of the animals were taken, and a three-dimensional model of the mandible was obtained from the two-dimensional images using the MIMICS 20.1 program. Length measurements were performed on the resulting 3D model. When the values measured in male and female rabbits were compared, it was determined that the length between the molars (B) was longer in females, and the corona length of the lower jaw teeth (I) was longer in males and was statistically significant ($p < 0.05$). It is thought that the 3D mandible model and measurements obtained in this study would be a resource for researchers working on experimental mandibular surgery in rabbits, would guide researchers as reference data in creating a rabbit model, would assist the physician in the clinic, and would help learn the anatomy of this region.

Keywords: Computer tomography; mandible; rabbit; 3D reconstruction

1 Introduction

Rabbits are considered analogous and suitable for clinical conditions, widely used for oral surgery and implantology testing. (Wang et al. 2023). The mandible of rabbits is larger than that of rats, and it is also an appropriate size when compared to other experimental animals and rodents. This makes surgical procedures less technically demanding, and it also facilitates rapid data acquisition with microcomputed tomography for applications performed on the mandible. Furthermore, this provides an experimental basis for jaw tissue engineering studies. Additionally, the cortical bone modulus and strength of rabbits are more similar to humans than other animals. Since it has sufficient volume, mandibular defects can be easily created. (Li et al. 2015; Baskin et al. 2021; Kim et al. 2023). The fact that rabbits are cheap and have a physiology comparable to humans in some respects increases their use. One of the rabbit's most important advantages is that it reaches skeletal maturity shortly after reaching sexual maturity at 6 months. (Akbulut et al. 2014, Campillo et al. 2014; Selçuk and Tıpırdamaz 2020).

Although the rabbit mandible is used as an experimental model in implant dentistry and cranio-maxillofacial surgery to evaluate specific tissue responses, tissue regeneration and biomaterial drug delivery in the cranio-maxillofacial region (Schlund et al. 2022), literature reviews on rabbit mandible data in healthy animals are very limited. This study was carried out to create three-dimensional (3D) models of the mandible using computed tomography (CT) images of a New Zealand rabbit and to reveal whether there were differences between genders.

2 Materials and Method

In the study, 12 healthy New Zealand rabbits (14 weeks old, 2580-3160 g) with the same care and feeding conditions, were used. The rabbits were obtained from euthanized animals as a result of a scientific study conducted at Karamanoğlu Mehmetbey University Faculty of Health Sciences.

The skulls of rabbits were scanned using a computerized tomography (Siemens, Somatom Sensation 64, Erlangen, Germany) device at 130 kVp, 300 mA, 330 msec and 0.5 mm slice thickness, and their images were obtained and saved in

DICOM (Digital Imaging and Communications in Medicine) format. Turgut et al. (2023) and Selcuk (2023) were used as references for the CT scan protocol. Three-dimensional modeling of the mandible was performed by importing CT images into MIMICS 20.1 (The Materialize Group, Leuven, Belgium). Morphometric measurements were performed on 3D images. Morphometric measurements and measurement points were determined using the relevant literature and were given in Table 1 and Figure 1 (Akbulut et al. 2014; Remzi et al. 2019). The nomenclature on the mandible was based on Nomina Anatomica Veterinaria (2017).

2.1 Statistical Analysis

The study's morphometric data analysis was performed using SPSS software version 21.0. The compliance of the variables to a normal distribution (histogram and probability graphs) and analytical methods (Kolmogorov-Smirnov/Shapiro-Wilk tests) were examined and it was determined that the data were parametric. Independent Samples t-test was used to compare the data obtained from female and male rabbits. Each gender was tested separately for correlations using Pearson Correlation coefficient calculations. Data are expressed as mean ± standard error (SE). $p<0.05$ was considered statistically significant.

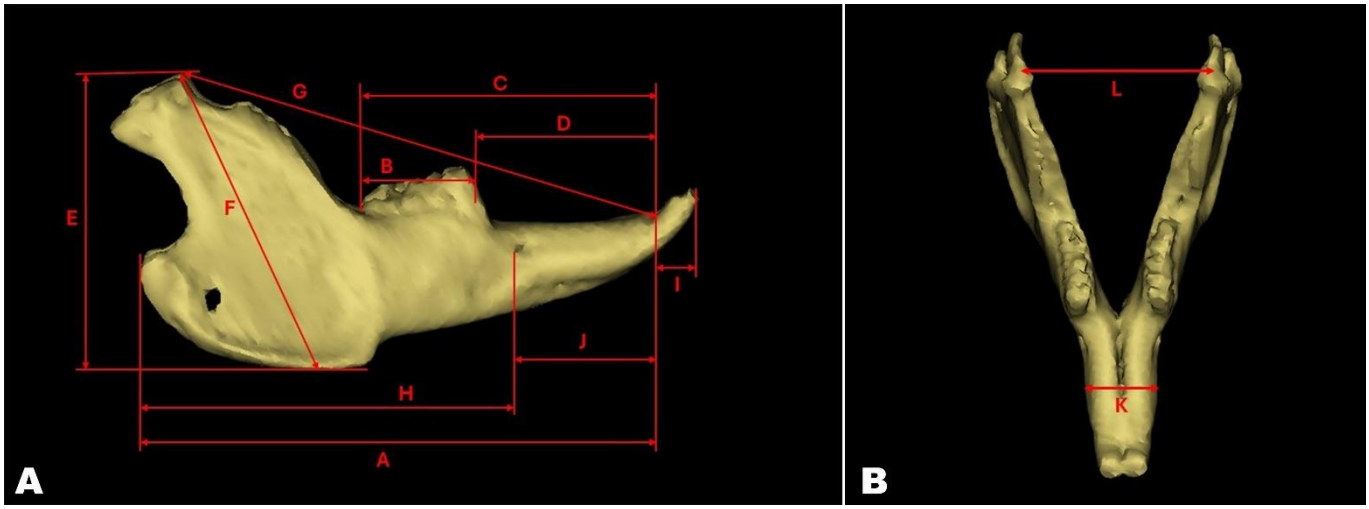

Fig. 1 A- Right side view of the mandible; **B-** Craniodorsal view of the mandible

Table 1 Mandible measurement points

Measurement	Measuring Points
A	Length between infradentale and gonion caudale
B	Length between molar teeth
C	The length between the infradentale and the alveolar aboral edge of the 3rd molar tooth
D	The length of the diastema (The length between the infradentale and the alveolar oral edge of the first premolar tooth)
E	Ramus mandibulae height (length between Gonion ventralis and the extreme point of processus condylaris)
F	The length between the plane passing parallel to the facies articularis of the processus condylare and the gonion ventrale
G	The length between infradentale and the extreme point of the processus condylare
H	The length between the caudal edge of the foramen mentale and the gonion caudale
I	Corona length of the mandibular tooth (The length between the tip of the mandibular incisive teeth and the tip of the alveolus of these teeth)
J	The length from incisor to oral border of foramen mentale
K	Width of mandibular body
L	Distance between left and right processus condylaris: measured from middle point

3 Results

Length measurements of the New Zealand rabbit mandible were given in Table 2, and correlation values of morphometric data were given in Table 3. When the measured values were compared for males and females, it was determined that the length between the molar teeth (B) was larger in females, and the corona length of the mandibular tooth (I) was larger in males and was statistically significant ($p<0.05$). No difference was detected between other measured length values ($p>0.05$).

In the correlation analysis in female rabbits, it was determined that A value was positively correlated with C, F, G, H and K values, D was positively correlated with F, G, H values, and H and K values were positively correlated ($p<0.05$). Additionally, it was determined that there was a strong positive correlation between C and D values, F and G, H values ($p<0.01$). When the values of male rabbits were examined, it was determined that A value showed a positive correlation with C, D, H values, C with J values, and J with D, G values ($p<0.05$). It was also determined that A and G values, C and D values had a strong positive correlation ($p<0.01$).

Table 2 Morphometric measurement values of the mandible obtained from 3D reconstruction

Measurement	Female	Male	p
A	62.553±1.146	61.468±0.978	0.488
B	14.077±0.218	14.803±0.217	**0.040***
C	34.972±0.572	34.838±0.629	0.879
D	20.953±0.422	20.470±0.514	0.484
E	38.297±0.482	39.330±0.595	0.207
F	40.435±0.590	41.255±0.569	0.341
G	59.720±1.349	57.748±0.993	0.267
H	44.512±0.862	44.655±0.398	0.883
I	5.875±0.269	4.713±0.116	**0.003***
J	14.700±0.198	14.527±0.473	0.742
K	10.422±0.238	10.447±0.085	0.923
L	31.587±0.504	32.408±0.393	0.229

*$p<0.05$; independent samples t test

Table 3 Correlation analyses of the mandible

	A	B	C	D	E	F	G	H	I	J	K	L
A	1	0.449	0.851*	0.810	0.131	0.880*	0.880*	0.916*	0.806	0.481	0.860*	-0.539
B	0.035	1	0.707	0.448	0.601	0.155	0.158	0.216	0.801	0.343	0.236	0.327
C	0.858*	0.359	1	0.936**	0.485	0.723	0.773	0.797	0.803	0.191	0.685	-0.420
D	0.876*	0.255	0.990**	1	0.486	0.833*	0.898*	0.882*	0.625	0.051	0.651	-0.636
E	-0.234	-0.756	-0.574	-0.521	1	0.237	0.240	0.200	0.458	-0.029	-0.127	0.189
F	0.304	-0.520	-0.148	-0.104	0.789	1	0.982**	0.985**	0.634	0.233	0.799	-0.731
G	0.963**	-0.058	0.786	0.836*	-0.161	0.370	1	0.987**	0.574	0.187	0.770	-0.781
H	0.897*	0.168	0.687	0.658	-0.199	0.374	0.793	1	0.652	0.187	0.858*	-0.769
I	0.352	-0.183	0.057	0.006	0.461	0.660	0.199	0.615	1	0.494	0.659	-0.059
J	0.780	0.276	0.842*	0.876*	-0.366	0.094	0.846*	0.527	-0.133	1	0.126	0.295
K	0.014	0.258	-0.165	-0.258	-0.113	0.069	-0.152	0.434	0.563	-0.446	1	-0.693
L	-0.146	0.644	-0.009	-0.148	-0.348	-0.290	-0.371	0.225	0.404	-0.358	0.780	1

*$p<0.05$, **$p<0.01$; Gray cells in the table are data for female New Zealand rabbits.

4 Discussion

Rabbit mandible is used as an experimental model in interventional applications such as dentistry and implants (Schlund et al. 2022; Kim et al. 2023). In this study, length measurements were made by three-dimensional modeling of the mandible on CT images in a healthy New Zealand rabbit.

In the study examining the effect of the gender factor in New Zealand rabbits, it was determined that the morphometric measurements of the mandible in male rabbits were larger than in female rabbits (Akbulut et al. 2014). The measured magnitude in male rabbits was not observed in our study. Akbulut et al. (2014) also found that the length between infradentale and gonion caudale was 66.62±3.32 mm in males and 66.15±2.10 mm in females (Akbulut et al. 2014). These values were found by Remzi et al. (2019) on mandible CT images of New Zealand rabbits as 62.260±0.224 mm in males and 66.960±0.224 mm in females. Similar results were obtained in our study. In Akbulut et al. (2014) study, they found that the length between the molar teeth was 16.55±0.44 mm in males and 16.28±0.56 mm in females, the length between the infradentale and the alveolar aboral edge of the 3rd molar was 38.24±1.31 mm in male rabbits and

38.01±1.36 mm in female rabbits, the length of the diastema was 21.97±1.02 mm in male rabbits and 21.51±0.92 mm in female rabbits, ramus mandibulae height was 44.86±1.79 mm in male rabbits and 44.82±2.11 mm in female rabbits, the length between the plane passing parallel to the facies articularis of the processus condylare and the gonion ventrale was 42.05±1.36 mm in male rabbits and 41.32±0.82 mm in female rabbits, the length between the caudal edge of the foramen mentale and the gonion caudale was 48.76±1.75 mm in male rabbits and 48.01±1.19 mm in female rabbits. In Remzi et al. (2019) study, these values were 15.740±0.266 mm, 35.060±0.127 mm, 19.780±0.232 mm, 37.020±0.245 mm, 40.000±0.289 mm, 46.100±0.216 mm in male rabbits and 16.260±0.266 mm, 38.160±0.127 mm, 21.960±0.232 mm, 41.180±0.245 mm, 42.760±0.289 mm, 47.280±0.216 mm in female rabbits, respectively. The findings of these two studies were consistent with the results of our study.

Akbulut et al. (2014) stated that the length between the infradentale and the extreme point of the processus condylare was 71.00±2.96 mm in males and 70.18±3.13 mm in females, and the corona length of the mandibular tooth was 13.89±3.75 mm in males and 12.97±1.81 mm in females. In our study, these values were found to be 57.748±0.993 mm and 5.875±0.269 mm in males, and 59.720±1.349 mm and 4.713±0.116 mm in females, respectively. In Remzi et al. (2019), it was found that the length from the incisor of the mental foramen to the edge of the mouth was 13.780±0.303 mm in males and 15.960±0.303 mm in females, the width of the mandibular body was 10.980±0.408 mm in males and 10.894±0.408 mm in females, the distance between the left and right processus condylaris was 26.740±0.662 mm in males and 28.260±0.662 mm in females. In our study, these values were 14.527±0.473 mm, 10.447±0.085 mm and 32.408±0.393 mm in males, and 14.700±0.198 mm, 10.422±0.238 and 31.587±0.504 mm in females, respectively. Upon comparing the data from two studies, while the measurements of the width of the mandibular body showed agreement, a discrepancy was observed between the length from the incisor of the mental foramen to the edge of the mouth and the distance between the left and right processus condylaris. The disparity in the studies was thought to have resulted from the age difference among the used rabbits.

In the length measurements Salih (2016) made on the mandibles of adult healthy rabbits, the length between the infradentale and the gonion caudale in males was 4.648±0.153 cm, the length between the caudal edge of the foramen mentale and the gonion caudale was 1.655±0.109 cm, and the length from the incisor of the foramen mentale to the edge of the mouth was 1.201±0.017 cm. stated that the width of the mandibular body was 0.955±0.143 cm and the distance between the left and right processus condylaris was 2.695±0.938 cm. These values in female rabbits were 5.248±0.133 cm, 2.178±0.098 cm, 1.202±0.032 cm, 1.068±0.140 cm, 2.968±0.079 cm, respectively. When these data were compared with our study, they showed incompatibility with the measurements of the length between the infradentale and gonion caudale and the distance between the left and right processus condylaris. It was thought that the current difference was due to age and breed differences.

In a study on male New Zealand rabbit mandibles using ultrasound, El-Bialy et al. (2003) stated that the height of the ramus mandible in healthy rabbits was 29.5±1.11 mm. In our study, this value was found to be 39.330±0.595 mm. It was thought that the current difference might be due to the difference in the method used and the inconsistency in the ages of the rabbits.

In a study in which no sexual dimorphism was performed by Borie et al. (2017) that used a caliper to evaluate different anatomical regions for implantation and oral surgery, the largest length of the mandible was 67.2±2 mm. In our study, these values were determined as 61.468±0.978 in male rabbits and 62.553±1.146 in female rabbits.

In a study conducted on New Zealand rabbits over two years old, without specifying gender, Monfared (2013) stated that the length of the foramen mentale from the incisor to the edge of the mouth was 18.9±0.4 mm, the length between the caudal edge of the foramen mentale and the gonion caudale was 53±4.3 mm, and the length between the infradentale and the gonion caudale was 75±5.5 mm. Our study found lower measurement values than reported in Monfared (2013) study, which we attributed to the use of younger rabbits.

In a study on adult female New Zealand rabbits, Campillo et al. (2014) reported that the diastema between the incisors and premolars was approximately 19 mm long. In our study, this value was 20.470±0.514 mm in male rabbits and 20.953±0.422 mm in female rabbits.

When the length measurements obtained as a result of our study were compared, it was concluded that they could not be used in sex discrimination of the New Zealand rabbit due to the small difference in morphometric values (Akbulut et al. 2014).

5 Conclusion

The use of three-dimensional anatomical models has increased with the development of methods such as microCT and MRI (Selcuk 2023). These methods, which use X-rays or a magnetic field, scan images of the bones, soft tissues, organs and vessels in the body from different angles and display them in sections (Dayan et al. 2019). With 3D models created from the images obtained, the structures of organs can be observed, measurements can be made, animal research models can be developed, and it helps the physician in the diagnosis of bone diseases and surgical operations (Haleem and Javaid 2019). It is anticipated that the 3D mandible model and measurements obtained in this study will be a resource for scientists working on experimental mandible surgery in rabbits, will guide researchers as reference data in creating a rabbit model, will assist the physician in the clinic, and will help in learning the anatomy of this region.

Acknowledgements

This research did not receive any specific grant from funding agencies in the public, commercial, or not-for-profit sectors.

Authors' contributions

MLS: conceptualization, methodology, investigation, writing original draft and editing.

Conflict of interest disclosure

The authors declare that they have no conflict of interest

References

Akbulut Y, Demiraslan Y, Gürbüz İ, Aslan K (2014) Yeni Zelanda tavşanı (Oryctolaguscuniculus L.)'ında cinsiyet faktörünün mandibula morfometrisine etkisi. Fırat Üniv Sağl Bil Vet Derg 28(1):15-18.

Baskin JZ, White BM, Vasanji A, Love TE, Eppell SJ (2021) Mandible biomechanics and continuously erupting teeth: a new defect model for studying load-bearing biomaterials. Biomedicines 9(7):730. doi:10.3390/biomedicines9070730

Borie E, Calzzani R, Dias FJ, Fuentes R, Salamanca C (2017) Morphometry of rabbit anatomical regions used as experimental models in implantology and oral surgery. Biomed Res J 28(12):5486-5472.

Campillo VE, Langonnet S, Pierrefeu A, Chaux-Bodard AG (2014) Anatomic and histological study of the rabbit mandible as an experimental model for wound healing and surgical therapies. Lab anim 48(4):273-277. doi:10.1177/0023677214540635

Dayan MO, Beşoluk K, Eken E, Aydoğdu S, Turgut N (2019) Three-dimensional modelling of the femur and humerus in adult male guinea pigs (guinea pig) with computed tomography and some biometric measurement values. Folia Morphol 78(3):588-594. doi:10.5603/FM.a2019.0002

El-Bialy T, El-Shamy I, Graber TM (2003) Growth modification of the rabbit mandible using therapeutic ultrasound: is it possible to enhance functional appliance results?. Angle Orthod 73(6):631-639.doi:10.1043/0003-3219(2003)073<0631:GMOTRM>2.0.CO;2

Haleem A, Javaid M (2019) 3D scanning applications in medical field: a literature-based review. CEGH 7(2):199-210. doi:10.1016/j.cegh.2018.05.006

Kim MK, Ham MJ, Kim WR, Kim HG, Kwon KJ, Kim SG, Park YW (2023) Investigating the accuracy of mandibulectomy and reconstructive surgery using 3D customized implants and surgical guides in a rabbit model. Maxillofac Plast Reconstr Surg 45(8):1-17. doi:10.1186/s40902-023-00375-9

Li Y, Chen SK, Li L, Qin, L, Wang XL, Lai YX (2015) Bone defect animal models for testing efficacy of bone substitute biomaterials. J Orthop Translat 3(3):95-104. doi:10.1016/j.jot.2015.05.002

Monfared AL (2013). Applied anatomy of the rabbit's skull and its clinical application during regional anesthesia. Glob Vet 10(6):653-7. doi:10.5829/idosi.gv.2013.10.6.72111

Nomina Anatomica Veterinaria (2017) International committee on veterinary gross anatomical nomenclature (6th ed. (Revised version)). Published by the Editorial Committee Hannover (Germany), Columbia, MO (USA), Ghent (Belgium), Sapporo (Japan).

Remzi OA, Caner B, Okan E, Ufuk K, Nuriye ÖK (2019) Accuracy and reliability of measurements obtained from 3-dimensional rabbit mandible model: a micro-computed tomography study. Acta Vet 69(2):192-200. doi:10.2478/acve-2019-0015

Salih QM (2016) Morphological and morph metric study of the mandible in the local Rabbits (Oryctolagus Cunicuius). Iraqi J Vet Med 40(1):25-29.

Selcuk ML (2023) Computed tomography reconstruction and morphometric analysis of the humerus and femur in New Zealand rabbits. Eurasian J Vet Sci 39(4):164-170. doi:10.15312/EurasianJVetSci.2023.413

Selçuk ML, Tıpırdamaz S (2020) A morphological and stereological study on brain, cerebral hemispheres and cerebellum of New Zealand rabbits. Anat, histol, embryol 49(1):90-96. doi:10.1111/ahe.12489

Schlund M, Depeyre A, Ranganath SK, Marchandise P, Ferri J, Chai F (2022) Rabbit calvarial and mandibular critical-sized bone defects as an experimental model for the evaluation of craniofacial bone tissue regeneration. J Stomatol Oral Maxillofac Surg 123(6):601-609. doi:10.1016/j.jormas.2021.12.001

Turgut N, Bahar S, Kılınçer A (2023) CT and cross-sectional anatomy of the paranasal sinuses in the Holstein cow. Vet Radiol Ultrasound 64(2):211-223. doi:10.1111/vru.13166

Wang Y, Zhang X, Mei S, Li Y, Khan AA, Guan S, Li X (2023) Determination of critical-sized defect of mandible in a rabbit model: Micro-computed tomography, and histological evaluation. Heliyon 9(7):e18047. doi:10.1016/j.heliyon.2023.e18047